

# Quantification of the Self-Excited Emotion Dynamics in Online Interactions

Yishan (Ivy) Luo<sup>1,2</sup>, Didier Sornette<sup>1</sup>, and Sandro Claudio Lera<sup>\*1,2,3</sup>

<sup>1</sup>Institute of Risk Analysis, Prediction and Management, Academy for Advanced Interdisciplinary Studies, Southern University of Science and Technology, Shenzhen, China

<sup>2</sup>School of Business, Southern University of Science and Technology, Shenzhen, China

<sup>3</sup>Connection Science, Massachusetts Institute of Technology, Cambridge, USA

## Abstract

Emotions are essential for guiding human behavior, particularly in social interactions. In modern societies, a growing share of human interactions are taking place online which has been shown to amplify and distort the expression and perception of emotions. However, the entanglement across different emotions is not fully understood. We use a multivariate Hawkes self-excited point process to model and calibrate the temporal expressions of six basic emotions in YouTube live chats. This allows us to understand interdependencies among emotions, but also to disentangle the influence from the video content and social interactions with peers. Positive emotions are found to be more contagious, while negative emotions tend to leave a longer-lasting impression on users' memories. Furthermore, we quantify the endogeneity of online emotion dynamics and find that peer interactions drive user emotional expressions 3-5 times more than passive content consumption. This underscores the powerful incentives of social interactions and the potential risk of emotional manipulation through the use of modern chatbots.

## Introduction

Emotions play a significant role in motivating human behaviors [1]. Social interactions are the main trigger for most emotions, and these emotions are conveyed through interpersonal communication [2]. Emotions thus facilitate interactions by creating emotional synchronization [3], and hence play a significant role in shaping collective narratives and influence fundamental societal issues such as political movements, public health campaigns, social justice initiatives, cultural trends, and community resilience in times of crisis [4, 5, 6].

In recent decades, there has been a significant increase in the proportion of human interactions occurring online. With advances in AI and the proliferation of online bots, it is becoming increasingly difficult to distinguish between humans and automated systems in online interactions [7, 8, 9]. This has prompted an active exploration of the role of emotions in digital engagements and its consequences for society. It has been shown that characteristics of the online environment, such as anonymity and the lack of non-verbal cues, amplify the expression and perception of emotions [10]. Emotional content on social media is more likely to be shared [11, 12]. Online users have been shown to favor emotionality over argument quality in information diffusion [13]. In particular, moral emotions increase the diffusion of political content in social networks [14]. Posts containing out-group animosity are significantly more likely to be shared on Facebook and Twitter [15]. The effects of “echo chambers” and heterogeneity of opinions both contribute to polarization online [16]. Furthermore, the emotion of online reviews is a reliable predictor of commercial success in various industries from movies to restaurants [17].

Despite widespread attention to the role of emotions on online platforms, we identify three limitations in the literature. First, there is a lack of consensus on the emotional responses on social platforms

---

\*Corresponding author

[18, 19]. Features that encourage favorable self-representation and social validation have been shown to induce a positivity bias [20, 21, 22]. At the same time, online interactions are driven by a cognitive negativity bias as illustrated by the disproportional focus on negative information [23, 24, 25]. Second, the study of online emotion diffusion has typically focused on the contagion of a single emotion, whereas interactions across different emotions have been less explored. Further, empirical evidence on the contagion effects of positive and negative emotions has been mixed [18]. Positive emotions have been shown to have larger contagion effects on social media platforms than negative ones [12, 26, 27]. Other evidence points to contagion effects in similar magnitudes for positive and negative emotions [28]. On the contrary, negative emotions, specifically anger, appear to be more contagious across social networks [29]. Third, it is unclear what type of online engagement influences the emotional states of users in what proportion. For instance, it has been shown that live comments during live events display amplified emotional intensity relative to regular comments [30]. However, the degree to which emotion intensity is influenced by live videos and peer interactions remains an unresolved question. More generally, it is a fundamental challenge to disentangle the effect of exogenous (exo) and endogenous (endo) influences in complex system dynamics [31].

We address these limitations by studying the co-evolution of 6 basic emotions in YouTube live chats. We represent emotions from the video content as exogenous triggers, and emotions from the live chats as endogenous ones. We then calibrate a multivariate self-excited conditional Hawkes point process [32, 33] to understand and disambiguate the influence of video content and prior live chats, as well as the interdependence across different states of emotions. By estimating the Hawkes model parameters across 397 videos spanning more than 780 hours of content, we find that peer social interactions contribute to user emotional expressions 3-5 times more than passive content consumption. In addition, the source of emotion intensity is attributed mainly to spontaneous user expressions rather than the video influence. This suggests that online emotions grow and spread more effectively through communication incentives and social interactions. Further, we find that positive emotions - especially joy - are more prone to contagion than negative ones. However, we identify a negativity bias in the temporal dynamics whereby users have a longer-lasting direct memory of negative emotions in online interactions. Our study provides practical implications for the design of social media and live-stream platforms. First, increasing user exposure to joyful content can diffuse positivity across social communities. Second, active communication channels - such as live chats or bots - can much more effectively engage users emotionally compared to passive ones - such as video advertisements.

## Results

### Live Chat Data

We examine the dynamics of emotions in online discussions through a collection of *YouTube Live* videos. YouTube is a video-sharing platform catered to a broad range of users across different cultures. YouTube Live allows the audience to chat with one another while the video is being played in real-time. We refer to the live discussions as *live chats* and a single user live comment as a *live chat message*, or just message. Videos with the *live chat replay function* record timestamped live discussions and allow viewers to retrieve the live experience by simultaneously replaying the video content and live chat messages. Figure 1(a) shows an example of a YouTube live video (left) with a live chat section (right) where viewers post messages visible to the entire audience as the video streams. Our sample includes 92,412 live chat messages across 397 videos, adding up to 780 hours of content and covering 27 topics (see SI Appendix for more statistics). Beyond messages, we also collect data of the video transcripts - or *subtitles* - which capture the video content.

Emotions from these texts are categorized by the widely adopted *6 basic emotions model* which includes joy, surprise, anger, disgust, fear, and sadness [34]. To this end, we fine-tune a Roberta transformer model that assigns emotion labels to each text [35]. The assignment is non-exclusive in the sense that each text can have multiple emotion labels (see Methods). An example is shown in Figure 1(b,c).

Our final dataset comprises 397 videos, each of which we represent by 12 event time-series. Specifically, for each emotion, there are two time-series: one annotating the occurrence of the emotion in

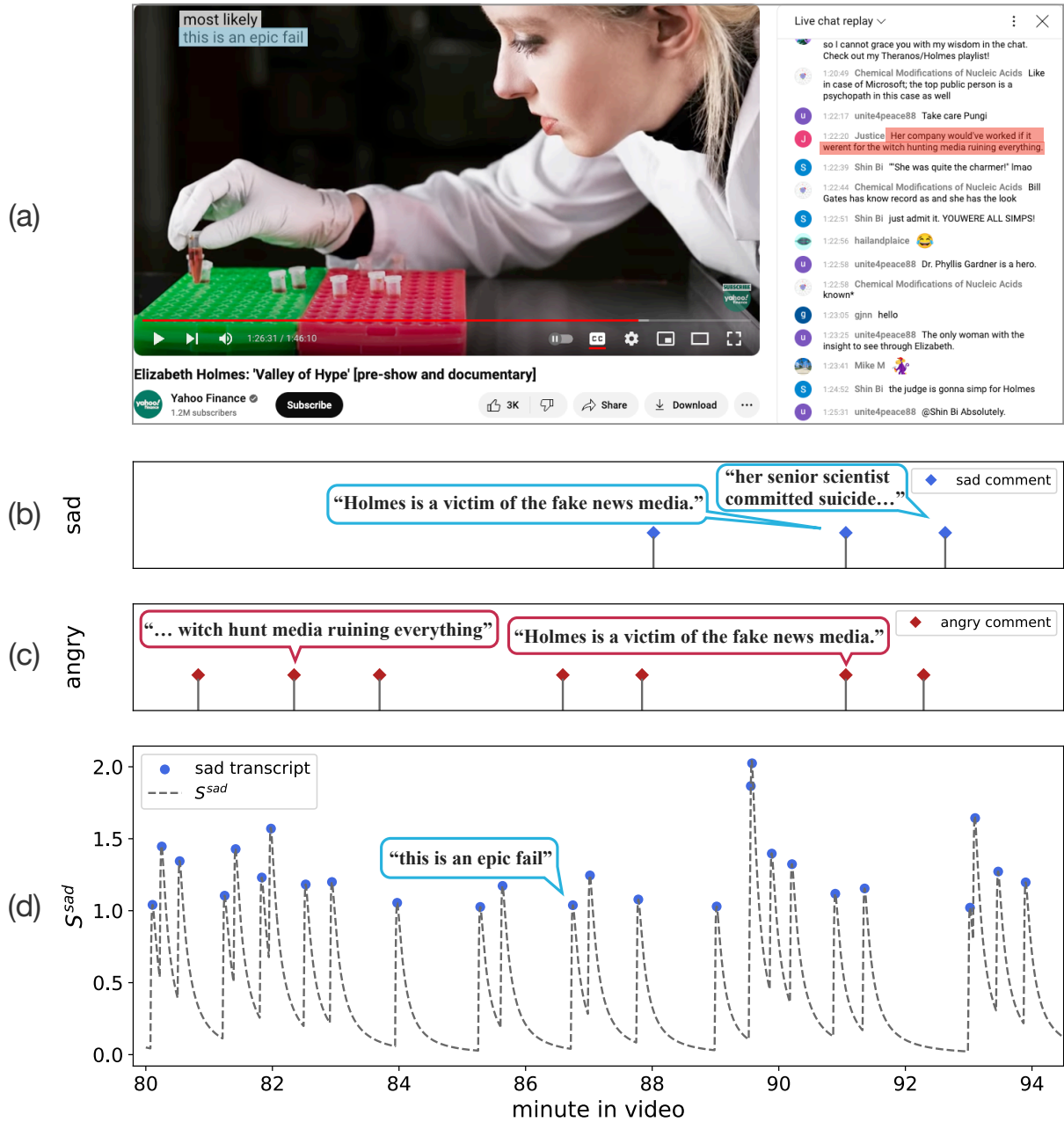


Figure 1: (a) Screenshot of a YouTube live video on the Theranos scandal involving Elizabeth Holmes with a live chat section on the right. The video content is captured by transcripts (*subtitles*), which we use to proxy exogenous emotional stimuli for the live chats. The live chat section displays timestamped messages from users reacting to the video content in real-time as the live video streams. We highlight an example of a transcript labeled as *sad* in blue, and a live chat message labeled as expressing *anger* in red. (b,c) We visualize the extraction of emotions from the video and live chat in the screenshot above. We plot the arrival of live chat messages that are labeled as *sad*, *angry*, indicated with diamond markers in blue, red. The shared x-axis shows the time in the video in units of minutes. The y-axis is unit-less. We label emotions non-exclusively. For instance, the sentence “Holmes is a victim of the fake news media” is labeled as both *sad* and *angry*. We assume these emotions are generated by the latent, inhomogeneous intensity defined by expression (1). (d) Time-varying component of the emotion *sad* in the video (transcript). Blue dots annotate the arrival of transcripts that are labeled as *sad*. The black dashed line shows our interpolation of the time-varying component.

the video subscript and the other in the live chat. Denote any of the six emotions by  $e \in \mathcal{E} \equiv \{ \text{joy, surprise, anger, disgust, fear, sadness} \}$ . Then, we denote by  $t_j^e$  the  $j$ -th time at which emotion  $e$  was observed in the live chat since the start of the video. Similarly, we denote by  $\tau_i^e$  the  $i$ -th time at which

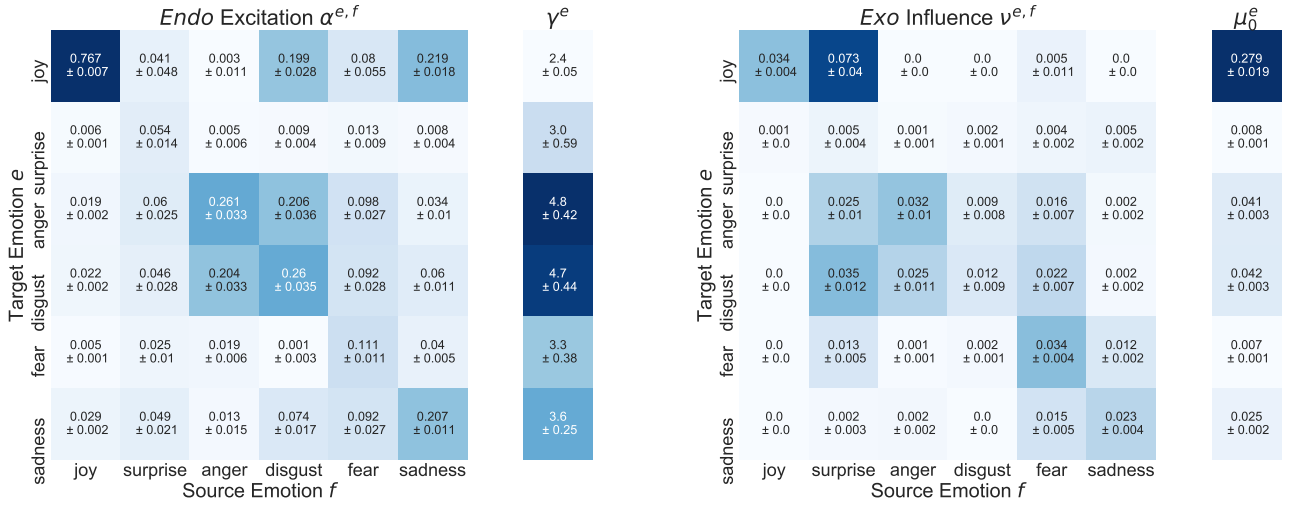


Figure 2: Visualizations of estimated parameters  $\nu^{e,f}$ ,  $\mu_0^e$ ,  $\alpha^{e,f}$ , and  $\gamma^e$  of the intensity defined by expression (1) from the maximisation of the log-likelihood function (5). The parameters are fitted ten times, each time sampling 60% (238) of the total 397 videos at random. Values and error bars are then obtained as sample mean and standard deviations across all 10 fits, respectively. Entry  $\alpha^{e,f}$  of the  $\alpha$  matrix represents excitation from emotion  $f$  to emotion  $e$  in the live chat, while  $\gamma^e$  represents the characteristic time-scale over which past emotions trigger new emotions  $e$ . The  $\nu$  matrix demonstrates how emotions in the video trigger emotions in the live chat, while  $\mu_0$  illustrates the spontaneous baseline intensity of spontaneous emotion expression.

emotion  $e$  was observed in the video subscript. We measure time in minutes from the start of the video. The median number of messages per video is 204 and the median time interval between two messages of the same emotion is 30 seconds. We refer to the SI Appendix for more summary statistics.

## Modeling Emotion Interactions with a Multivariate Hawkes self-excited Conditional Point Process

Emotions are contagious [36]. We therefore propose to describe the arrival of  $|\mathcal{E}| = 6$  different emotions as  $|\mathcal{E}|$ -dimensional self- and cross-exciting Hawkes point processes [37]. Hawkes point processes have been used to study self-exciting phenomena such as earthquakes [38], financial trades [39, 40], video viewing activities, [41], and information cascades [42]. The point process describes the statistical occurrence of different types of emotions, also called *events*. For a given emotion  $e \in \mathcal{E}$ , we distinguish two types of events: emotion  $e$  is present in (the subscript of) the video content or emotion  $e$  is present in the live chat. It is our goal to understand to what extent a given emotion  $f \in \mathcal{E}$  triggers another emotion  $e \in \mathcal{E}$  either exogenously from the video to the live chat or endogenously from live chats to live chats. Here the adjectives exogenous and endogenous refer to the point of view of the live chat. We assume that emotions in the live chat cannot influence emotions in the video. This is precisely the case if the video is pre-recorded (e.g. a documentary, as in Figure 1), and approximately the case where the video involves a live streamer which could potentially interact with the viewers.

The time series  $\{t_j^e\}$  of observed live chats of emotion  $e$  is assumed to be sampled from a latent, inhomogeneous event intensity  $\lambda^e(t)$ . This intensity is influenced by three factors: (i) a homogeneous base-rate  $\mu_0^e$  which captures live chat messages of emotion  $e$  that are spontaneously posted by users in the absence of any influence from the video or live chat; (ii) an inhomogeneous rate  $\mu_1^e(t)$  which captures live chat messages of emotion  $e$  that are posted due to an influence from the video; (iii) finally, there is an endogenous rate accounting for the fact that past live chat messages trigger new ones. This is represented in the following expression for the intensity of emotion  $e \in \mathcal{E}$  as a Hawkes

point process:

$$\lambda^e(t) = \underbrace{\mu_0^e}_{\text{exo base rate}} + \underbrace{\sum_{f \in \mathcal{E}} \nu^{e,f} S^f(t)}_{\text{exo video influence } \mu_1^e(t)} + \underbrace{\sum_{f \in \mathcal{E}} \sum_{t_j^f < t} \phi^{e,f}(t - t_j^f)}_{\text{endo chat influence}}. \quad (1)$$

The intensity is defined such that  $\lambda^e(t)dt$  is the probability that an emotion  $e$  occurs in the live chat between  $t$  and  $t + dt$ . Equation (1) states that the intensity at which emotions of type  $e$  are generated in the live chat is an additive function of past emotions. The term  $\mu_0^e$  is just a constant as described above. The term  $S^f(t)$  is the time-varying presence of emotion  $f$  in the video subscript (see Methods for details and Figure 1(d) for an example of  $S^{\text{sad}}(t)$ ). The term  $\nu^{e,f} S^f(t)$  then represents the rate at which emotion  $f$  in the video triggers emotion  $e$  in the live chat. For instance, a sad scene in the video can trigger an angry message in the live chat. Summing over all emotions  $\mathcal{E}$  we arrive at the rate  $\mu_1^e(t)$  by which any emotion from the video triggers emotion  $e$  in the live chat. The third term captures the endogenous influence from prior live chat messages. Here,  $\phi^{e,f}(t - t_j^f)$  represents the influence of an emotion  $f$  at time  $t_j^f$  on emotion  $e$  at time  $t$ . The intensity kernel  $\phi^{e,f}(\cdot)$  is monotonously decaying, such that the more time has passed, the less of an influence a prior message has. We follow the common assumption that  $\phi$  is exponential, that is  $\phi^{e,f}(t) = \alpha^{e,f} \frac{1}{\gamma^e} e^{-\frac{1}{\gamma^e} t}$  with decay time  $\gamma^e$ . The larger  $\gamma^e$  is, the longer the direct memory of a past live chat message has on emotion  $e$ . We assume that  $\gamma^{e,f} \equiv \gamma^e$  for simplicity. The coefficient  $\alpha^{e,f}$  represents the endogenous excitation effect from emotion  $f$  to emotion  $e$  in the live chat.

In summary, the intensity  $\lambda^e(t)$  from Equation (1) is parametrized by a set of  $2|\mathcal{E}| + 2 = 14$  parameters: the exogeneous rate  $\mu_0^e$ , the decay time  $\gamma^e$ , as well as  $|\mathcal{E}|$  parameters for  $\nu^{e,f}$  and  $\alpha^{e,f}$ , respectively. We estimate these parameters by maximizing their log-likelihood functions (see Methods). Since each emotion has its own intensity  $\lambda^e$ , our model has a total of  $|\mathcal{E}|(2|\mathcal{E}| + 2) = 84$  parameters. However, the estimation of the different  $\lambda^e$  are decoupled from each other, so that we can estimate each set of 12 parameters separately. The fitted parameters are visualized in Figure 2 and discussed below.

## Quantifying Exogenous and Endogenous Influences

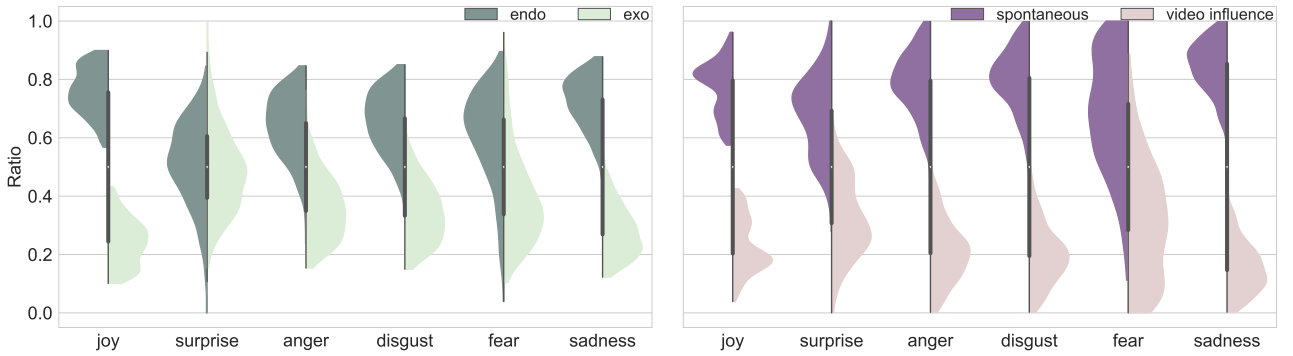


Figure 3: (a) For each video, we calculate the average ratio of endogenous (exogenous) intensity to the total intensity across time. Plot (a) shows the distribution of these ratios across videos. We notice that emotions are predominantly triggered endogenously. (b) Same as plot (a) but for the ratio of spontaneous (video influenced) intensity to total exogenous intensity.

Videos provide a shared experience among viewers, giving rise to amplified emotion intensities during live broadcasting events [30]. However, it is unclear whether the emotional experience and amplification stem from the live videos themselves or the interactions among peers [30]. The Hawkes framework (1) allows us to answer this question by comparing exogenously and endogenously triggered events. The exogenous (exo) component,  $\mu^e(t) = \mu_0^e + \mu_1^e(t)$ , represents influences from the video content and elsewhere. The endogenous (endo) component,  $\sum_{f \in \mathcal{E}} \sum_{t_j^f < t} \phi^{e,f}(t - t_j^f)$ , captures the



influence from prior live chat messages and hence stems from interactions with peers. At any given time, we can determine the fraction of exo-influence as  $R_{\text{exo}}^e(t) = \mu^e(t)/\lambda^e(t)$  and the ratio of endo influence as  $R_{\text{endo}}^e(t) = 1 - R_{\text{exo}}^e(t)$  where all quantities are calculated with the estimated parameters (Figure 2). Subsequently, we calculate the average exo- and endo-ratios,  $\langle R_{\text{exo}}^e \rangle$  and  $\langle R_{\text{endo}}^e \rangle$ , of a given video by averaging across all times events take place. Figure 3 (left) shows the distribution of these quantities over all videos in our sample. We observe that, despite the constant exogenous influence from video feeds, endogenous influence dominates the emotion dynamics across emotion types. This demonstrates that emotional expressions in live discussions are disproportionately driven by social interactions with active participants rather than passive video content consumption. In particular, we see that the emotion of joy has the highest ratio of endogenous influence, being 80% driven by prior participants. In contrast, and in accordance to common sense, the emotion of surprise is the most responsive to exogenous stimuli where roughly 50% of the total intensity is triggered exogenously.

Similarly, we can calculate the ratio of purely exogenous spontaneous emotions relative to video-induced emotions, that is  $R_0^e = \mu_0^e/(\mu_0^e + \mu_1^e(t))$  and its complement  $R_1^e = 1 - R_0^e$ . Figure 3 (right) shows the distribution of  $\langle R_0^e \rangle$  versus  $\langle R_1^e \rangle$  over the set of all videos. The rates of chats induced by videos is typically one-fourth the rate of spontaneous chats. We note, however, that there is significant heterogeneity across video categories (SI Appendix).

In summary, these results suggest that participants use YouTube live videos more as a platform for expressing their opinions and emotions than for engaging with the content itself.

## Emotion Contagion and Interaction Dynamics

We now interpret the estimated parameters from Equation (1) visualized in Figure 2.

Above, we have seen that the majority of the live chat messages are triggered endogenously. An alternative way to confirm this high level of endogeneity is directly via the estimated *branching ratio matrix*  $\alpha^{e,f}$ . The branching ratio matrix quantifies the interaction between different event types within the process. The branching ratio matrix is a square matrix where each element represents the expected number of type  $e$  emotional events directly triggered by a type  $f$  emotional event. The diagonal elements of the branching ratio matrix represent the self-excitation within the same emotion. The off-Diagonal elements capture cross-excitation, where an emotional event of type  $f$  increases the likelihood of an emotional event of type  $e$ . The sum  $\sum_e \alpha^{e,f}$  represents the expected number of offspring events generated by a single parent event of type  $f$ . If this sum exceeds 1 for any event type, it implies a supercritical process for that type, leading to potentially explosive behavior (more and more events). Another important quantity is the spectral radius of the branching ratio matrix, defined as the largest absolute value of its eigenvalues. It gives an overall measure of the system's tendency toward self-excitation and cross-excitation. If the spectral radius is smaller than 1, the system is subcritical, meaning that the process is stable, and the number of events will not grow indefinitely. The influence of past events decays over time. This is the relevant regime found in Figure 2 with a spectral radius equal to 0.8. Examining the entries of the branching ratio matrix shown in Figure 3 (left), we find that online emotion dynamics are driven 3-5 times more by social interactions than by exogenous influences. We thus henceforth focus on the endogenous parameters  $\alpha^{e,f}$  and  $\gamma^e$ .

Zooming in on the entries of the  $\alpha^{e,f}$  matrix reveals that each of the 6 emotions displays distinct temporal dynamics (Figure 2, left). One can readily notice that joy has significantly higher levels of self-excitation rate than other emotions as shown by the comparison between the different diagonal entry  $\alpha^{e,e}$  representing self-excitation. Quantitatively, positivity is up to 3 times more contagious than even the high-arousal negative emotions of anger and disgust. The fact that surprise is the least contagious of all the emotions serves as a useful consistency check. Similarly, fear shows relatively low levels of excitation.

Generally, self-excitation dominates over cross-excitations that are quantified by the off-diagonal values  $\alpha^{e,f}$  representing the influence of emotion  $f$  on emotion  $e$ . A notable exception is the moral emotions of anger and disgust which are mutually reinforcing in almost equal magnitudes. It is also noteworthy that all of the emotions, but particularly disgust and sadness, trigger joy. We will come back to these observations in the Discussion section below.

Recall that the decay times  $\gamma^e$  characterize the direct time scale over which past emotions trigger

future ones of type  $e$ . Figure 3 shows that users have a significantly longer direct memory of negative emotions, in particular of the high-arousal emotions of anger and disgust. Coupled with the fact that emotions are triggered primarily through self-excitation, this suggests that negative emotions impose a more lasting direct influence on future interactions and the emotional state of users.

## Discussion

Across 92,412 live chat messages on YouTube, we find that, despite stimulative inputs from the video, online emotions are driven more by endogenous user interactions by a factor of 3 to 5. The dynamics of emotions are primarily driven by the incentives for peer communication and are further amplified through social interactions. Our results show that endogenous user interactions are the main contributors to online emotion expressions, which has been found to be consistent predictors for user engagement on video platforms [43, 44]. This provides empirical evidence that emotions are inherently communicative, being both evoked by social interactions and expressed through communication [2]. We find that live videos, while serving as the primary medium for content delivery, have only a limited direct impact on user discussions, which largely arise spontaneously. However, live videos play a crucial role in creating a shared experience that fosters empathy and enhances social interactions [3].

By quantifying the excitation and temporal decay of different emotions in online interactions, we show that positivity is more contagious whereas negative emotions create a more enduring impact on users' memory. This reconciles mixed findings on online emotion propagation by identifying different pathways for positive and negative emotions to spread across online platforms. We further quantify an intrinsic joyful bias in users' heightened propensity for spontaneous expressions of joy. Our results suggest that positivity bias [20, 21, 22] and negativity bias [23, 24, 25] coexist on different dimensions of social platform interactions. Users are positively biased in the spontaneous expression of emotions, and yet negatively biased in the perception of emotions.

While self-excitation dominates, anger and disgust cross-excite one another in comparable magnitudes in online interactions. It may be, however, that this result is partially explained by the frequent co-labeling of anger and disgust in the same text (see SI Appendix). Either way, the strong self- and cross-excitation of these high arousal negative emotions can explain the frequent occurrence of large-scale moral outrage in online conversation [45], and hence contributes to increased divisiveness and polarization [46, 47].

We further observe interaction effects across positive and negative emotions. In particular, both disgust and sadness trigger joy in online interactions. Such patterns can be observed in trolling and anti-social behaviors online. Individuals are less restrained online and trolling behaviors are prevalent on social platforms [48, 49]. Prior trolling activities can further trigger trolling behavior in future interactions [50].

A notable limitation of our analysis is that it is only text-based. Future studies incorporating multi-modal inputs will allow us to understand different emotion dynamics across communication channels. We also do not distinguish human participants from bots and automated accounts in YouTube live chats. Such a distinction would allow for a direct generalization of our methodology. Motivated by the growing capability of LLMs to simulate human emotions and infiltrate online environments, future studies are needed to better understand the emotional exchange between humans and modern chatbots.

## Conclusions

Using 92,412 YouTube live chat messages across 397 videos, we found that interactions among users are 3-5 times more emotionally contagious than passive video content. In particular, positivity is more contagious whereas negativity is more memorable. Such understanding of online emotion dynamics has practical implications for the design of social platforms. First, user engagement is more effectively facilitated through interactive features than passive content. Second, promoting joyful content can effectively spread positivity, while the promotion of negative emotions can have lasting and alarming consequences, such as provoking moral outrage. Moreover, with the increasing ability of large language

models (LLMs) to simulate human emotions [51], our results highlight the significant potential threat posed by internet bots in manipulating collective emotions through user interactions, which could potentially disrupt social order.

## Methods

### Collecting YouTube Live Chats

We examine emotion dynamics in YouTube live videos with replay functionality across 27 topics (see SI Appendix for the complete list). We first compile the list of keywords and collect completed live video IDs for each keyword using the keyword search function via YouTube API in Python.<sup>1</sup> Subsequently, we retrieve the video transcript and live chat messages for each video respectively. We use the ChatDownloader package<sup>2</sup> to retrieve the available timestamped live chat content, and the YouTube-transcript-API<sup>3</sup> to retrieve the video transcript. We then only retain videos with a median time difference between two subsequent live chat messages between 1 second and 5 minutes. We exclude videos where over 70% of live chat messages are non-English. For the remaining videos, we remove live chat messages that are not in English. For each video, we also remove any live chat messages that occur before the first or after the last transcript arrival time. This leaves us with a total of 673,551 live chat messages across 1,957 videos.

### Labeling Emotions in Text

<b>Original</b>	joy	anticipation	optimism	love	trust	sadness	pessimism	anger	disgust	fear	surprise
<b>Mapped</b>	joy	joy	joy	joy	joy	sadness	sadness	anger	disgust	fear	surprise

Table 1: We fine-tune a transformer model to detect the presence of 6 basic emotions in text. Originally, our training data contained 11 emotion labels, we mapped the 11 emotions to 6 basic emotions prior to training according to this Table.

We consider expressions of emotions through text. We characterize emotions with the widely adopted “6 basic emotions model” [34]. These basic emotions are  $\mathcal{E} \equiv \{ \text{joy, surprise, anger, disgust, fear, sadness} \}$ . Multiple emotions can arise simultaneously in a single sentence [52, 53]. We thus want to assign to each text a vector of length 6 indicating the non-exclusive presence of each of the six emotions. This amounts to a multi-label classification problem. For training data, we rely on the SemEval-2018 dataset containing 6,838 Tweets with non-exclusive emotion labels across 11 emotions [54]. We map these 11 emotions to our 6 emotions via Table 1. Subsequently, we fine-tune a Roberta transformer model [35]. The transformer takes as input a text and gives as output the probabilities for each of the 6 basic emotions via 6 independent sigmoid activations. We use the binary cross-entropy loss function for training. During prediction, we convert each sigmoid output to a binary indicator at the 0.5 cutoff. This allows us to assign to each live chat message and video subscript a subset of emotions in  $\mathcal{E}$  (e.g. Figure 1).

For each video and emotion, we calculate the average number of live chat messages per minute. To avoid outlier or otherwise irregular live chats, we only retain videos for which this average lies within the 20<sup>th</sup>- and 80<sup>th</sup>-quantile across all videos. This gives us a final sample of 92,412 live chat messages across 397 videos, which amounts to a total of 780 hours. The median duration of a video is 107 minutes and the median number of live chat messages per video is 204. Across all videos, the median number of live chat messages per minute is 1.63 for joy, 0.17 for disgust, 0.16 for anger, 0.11 for sadness, 0.03 for fear, and 0.03 for surprise. We refer to the SI Appendix for additional statistics.

<sup>1</sup><https://developers.google.com/YouTube/v3>

<sup>2</sup><https://github.com/xenova/chat-downloader>

<sup>3</sup><https://pypi.org/project/YouTube-transcript-api/>



## Parametrization of Video Influence

As elaborated above, we model the arrival of emotions as a bi-hexivariate Hawkes process given by expression (1). For emotion  $e \in \mathcal{E}$ , within a given live chat session, we observe  $N^e$  events, with the  $j^{\text{th}}$  event taking place at time  $t_j^e$ . We define  $t_0^e \equiv 0$ ,  $t_{N^e+1}^e \equiv T$  where  $T$  is the video duration. This way, the observation period over the entire process is  $\{t_i^e \mid i = 0, \dots, N^e + 1\}$ . Similarly, we denote by  $\tau_i^e$  the time at which the  $i$ -th subscript of emotion  $e$  appears in the video. We measure time in units of minutes.

Prior studies have shown that assuming the exogenous influence  $\mu^e(t)$  to be constant may lead to false attribution to endogenous effects [55, 40]. The YouTube live videos provide us with the unique opportunity to observe a time-varying influence of the video content on user discussions. We use the video transcript to capture the time-varying emotional content of the video. For instance, it is reasonable to assume that a particularly sad scene in the video induces sad emotions in the live chat. Further, one can expect cross-influence, e.g. that a sad scene in the video induces angry emotions in the live chat (Figure 1). In particular, this is to be distinguished from a sad scene in the video triggering a sad message in the live chat, which in turn triggers either a sad or angry message. To capture such cross-influence from the videos, we parameterize the exogenous intensity of emotion  $e$  as

$$\mu^e(t) = \mu_0^e + \mu_1^e(t) \equiv \mu_0^e + \sum_{f \in \mathcal{E}} \nu^{e,f} S^f(t), \quad (2)$$

where  $\mu_0^e$  is a time-invariant, unobserved baseline intensity of spontaneous expression of emotion  $e$  in the absence of influence from video or prior live chat messages. By contrast, we denote by  $S^f(t)$  the time-varying intensity of emotion  $f$  in the video, and  $\nu^{e,f}$  the cross-influence from emotion  $f$  in the video to emotion  $e$  in the live chat. The term  $\nu^{e,f} S^f(t)$  is thus the time-varying intensity at which emotions of type  $f$  in the video trigger emotions of type  $e$  in the live chat.

The intensity  $S^f(t)$  is given by  $S^f(t) = \sum_{\tau_j^f < t} s_{\tau_j^f}^f(t)$  where  $\{\tau_j^f\}$  enumerates all times at which a subtitle of emotion  $f$  first appears in the video. Here,  $s_{\tau_j^f}^f(t)$  captures the time-varying influence of a video subtitle of emotion  $f$  appearing in the video at time  $\tau_j$ . Clearly,  $s_{\tau_j^f}^f(t) = 0$  for  $t < \tau_j$ . In order to incorporate the video impact, we need to make reasonable assumptions on the shape of the temporal dependence of the influence of emotions in the video on emotions in the live chat. It is natural to assume that it takes a few seconds for the audience to process the transcript and react. We also expect the influence of the video to peak after a rapid increase in intensity and then fade out with time. Empirical evidence demonstrates that information retention in humans decays with a fat tail, i.e. slower than an exponential [56]. To approximately capture the rapid initial increase and subsequent slow decline, we use the log-normal function to parametrize the memory of a subscript in the video:

$$s_{\tau_j}^f = \frac{1}{\sqrt{2\pi}\sigma(t - \tau_j)} \exp\left(-\frac{(\ln(t - \tau_j) - \mu)^2}{2\sigma^2}\right). \quad (3)$$

Under a finite range of the variable that depends on  $\sigma$ , the log-normal function exhibits shapes similar to a power law [57], while also displaying an initial steep increase.

To fix  $\mu$  and  $\sigma$ , we assume that the intensity of each transcript peaks 2 seconds after appearance, and that 50% of the emotion intensity for each transcript is manifested within 10 seconds of transcript appearance. In other words, we assume that the maximum of the log-normal function lies at 2 seconds,  $\exp(\mu - \sigma^2) = 2$ , and that the median is equal to 10 seconds,  $\exp(\mu) = 10$ . Numerically solving for  $\mu$  and  $\sigma$  yields 2.3 and 1.3 respectively in units of minutes. To ensure that our results are not strongly dependent on this choice of  $\mu$  and  $\sigma$ , we have checked that our results remain qualitatively similar for different values and functional shapes (see SI Appendix). Alternatively, these parameters could be directly fitted from the data, a task which we leave for future research.

In summary, the shape  $S^f(t)$  is a sum of log-normal functions, with local peaks at 2 seconds after the appearance of a new subtitle of emotion  $f$ . An example of  $s^{\text{sad}}$  is shown in Figure 1(d). We further stress that our framework is different from the typical multivariate Hawkes process in that expression (2) contains cross-influence terms from different exogenous sources. This is because we condense a bi-hexivariate Hawkes model containing two systems of events into one multivariate Hawkes self-excited

conditional point process. This specification is therefore necessary to distinguish video-based emotion events and chat-based emotion events.

## Fitting the Parameters of the Hawkes Process

A general representation of the log-likelihood of intensity  $\lambda^e$  from (1) is given by

$$\log(L^e) = \sum_{i=1}^{N^e} \log(\lambda^e(t_i^e)) - \int_0^T ds \lambda^e(s) \quad (4a)$$

$$= \sum_{i=1}^{N^e} \log(\lambda^e(t_i^e)) - \int_0^T ds \mu^e(s) - \sum_{f \in \mathcal{E}} \sum_{t_j^f} \int_{t_j^f}^T ds \phi^{e,f}(s). \quad (4b)$$

We follow the common assumption that  $\phi$  is exponentially decaying and write  $\phi^{e,f}(t) = \alpha^{e,f} \frac{1}{\gamma^e} e^{-\frac{1}{\gamma^e} t}$  with decay time  $\gamma^e$ , such that (4b) can be expanded into

$$\log L^e \left( \mu_0^e, \nu^{e,f}, \alpha^{e,f}, \gamma^e \right) = \sum_{i=1}^{N^e} \log \left( \mu_0^e + \sum_{f \in \mathcal{E}} \nu^{e,f} S^f(t_i) + \sum_{f \in \mathcal{E}} \sum_{t_j^f < t} \alpha^{e,f} \frac{1}{\gamma^e} e^{-\frac{1}{\gamma^e}(t_i - t_j^f)} \right) - \mu_0^e T - \sum_{f \in \mathcal{E}} \nu^{e,f} M_1^f + \sum_{f \in \mathcal{E}} \sum_{t_j^f} \alpha^{e,f} \left( e^{-\frac{1}{\gamma^e}(T - t_j^f)} - 1 \right), \quad (5)$$

where  $M_1^f \equiv \int_0^T ds S^f(s)$  is a constant that we calculate numerically. A detailed derivation of Equation (5) is found in the SI Appendix.

We estimate values for  $\mu_0^e$ ,  $\nu^{e,f}$ ,  $\alpha^{e,f}$ , and  $\gamma^e$  by maximizing Equation (5) via Quasi-Newton optimization. We use the ‘‘L-BFGS-B’’ optimization algorithm from the family of quasi-Newton methods to handle bound constraints. The variable bound constraints are specified as follows:  $0 \leq \alpha \leq 50$ ,  $10^{-6} \leq \nu \leq 10$ ,  $0.1 \leq \gamma \leq 20$ ,  $0 \leq \mu \leq 50$ .

Note that Equation (5) represents the log-likelihood for a single video,  $\log L^e = \log L_k^e$  where  $k$  enumerates the videos in our data sample. We thus aggregate  $L_k^e$  across all videos and estimate the model parameters by maximizing  $\sum_k \log L_k^e$ . The total number of parameters is  $2|\mathcal{E}| + 2 = 14$  per emotion. This amounts to a total of  $|\mathcal{E}|(2|\mathcal{E}| + 2) = 84$  parameters to be estimated for  $|\mathcal{E}| = 6$  emotions. However, the parameters for each emotion can be estimated independently because there is no interdependence between the parameters across different emotion types. This gives rise to six independent fits of 14 parameters each. To verify that the obtained fits are valid, we first test our model with synthetically generated data and obtain reliable performance (see SI Appendix). We also refer to the SI Appendix for additional robustness checks with respect to different parametrizations and subsets of emotions. To mitigate potential biases from Simpson’s paradox, where combining individual groups may lead to spurious trends, we estimate our model parameters using bootstrapped samples. We bootstrap our data 10 times, each time sampling only 60% of all available videos. This allows us to estimate the parameters as averages across bootstrapped samples and we use standard deviations as error bars. The fitted parameters are shown in Figure 2.

## References

- [1] Paul D MacLean. *The triune brain in evolution: Role in paleocerebral functions*. Springer Science & Business Media, 1990.
- [2] Peter A Andersen and Laura K Guerrero. Principles of communication and emotion in social interaction. In *Handbook of Communication and Emotion*, pages 49–96. Elsevier, 1996.
- [3] Lauri Nummenmaa, Enrico Glerean, Mikko Viinikainen, Iiro P Jääskeläinen, Riitta Hari, and Mikko Sams. Emotions promote social interaction by synchronizing brain activity across individuals. *Proceedings of the National Academy of Sciences*, 109(24):9599–9604, 2012.
- [4] Nicholas A Valentino, Ted Brader, Eric W Groenendyk, Krysha Gregorowicz, and Vincent L Hutchings. Election night’s alright for fighting: The role of emotions in political participation. *The Journal of Politics*, 73(1):156–170, 2011.
- [5] Amit Goldenberg, David Garcia, Eran Halperin, and James J Gross. Collective emotions. *Current Directions in Psychological Science*, 29(2):154–160, 2020.
- [6] Johannes C Eichstaedt, Garrick T Sherman, Salvatore Giorgi, Steven O Roberts, Megan E Reynolds, Lyle H Ungar, and Sharath Chandra Guntuku. The emotional and mental health impact of the murder of george floyd on the us population. *Proceedings of the National Academy of Sciences*, 118(39):e2109139118, 2021.
- [7] Massimo Stella, Emilio Ferrara, and Manlio De Domenico. Bots increase exposure to negative and inflammatory content in online social systems. *Proceedings of the National Academy of Sciences*, 115(49):12435–12440, 2018.
- [8] Fatimah Ishowo-Oloko, Jean-François Bonnefon, Zakariyah Soroye, Jacob Crandall, Iyad Rahwan, and Talal Rahwan. Behavioural evidence for a transparency–efficiency tradeoff in human–machine cooperation. *Nature Machine Intelligence*, 1(11):517–521, 2019.
- [9] Mayada Oudah, Kinga Makovi, Kurt Gray, Balaraju Battu, and Talal Rahwan. Perception of experience influences altruism and perception of agency influences trust in human–machine interactions. *Scientific Reports*, 14(1):12410, 2024.
- [10] Amit Goldenberg and Robb Willer. Amplification of emotion on social media. *Nature Human Behaviour*, 7(6):845–846, 2023.
- [11] Junhan Chen, Yumin Yan, and John Leach. Are emotion-expressing messages more shared on social media? A meta-analytic review. *Review of Communication Research*, 10, 2022.
- [12] Emilio Ferrara and Zeyao Yang. Quantifying the effect of sentiment on information diffusion in social media. *PeerJ Computer Science*, 1:e26, 2015.
- [13] Jason Weismueller, Paul Harrigan, Kristof Coussement, and Tina Tessitore. What makes people share political content on social media? The role of emotion, authority and ideology. *Computers in Human Behavior*, 129:107150, 2022.
- [14] William J Brady, Julian A Wills, John T Jost, Joshua A Tucker, and Jay J Van Bavel. Emotion shapes the diffusion of moralized content in social networks. *Proceedings of the National Academy of Sciences*, 114(28):7313–7318, 2017.
- [15] Steve Rathje, Jay J Van Bavel, and Sander Van Der Linden. Out-group animosity drives engagement on social media. *Proceedings of the National Academy of Sciences*, 118(26):e2024292118, 2021.
- [16] Jürgen Buder, Lisa Rabl, Markus Feiks, Mandy Badermann, and Guido Zurstiege. Does negatively toned language use on social media lead to attitude polarization? *Computers in Human Behavior*, 116:106663, 2021.

- [17] Matthew D Rocklage, Derek D Rucker, and Loran F Nordgren. Mass-scale emotionality reveals human behaviour and marketplace success. *Nature Human Behaviour*, 5(10):1323–1329, 2021.
- [18] Amit Goldenberg and James J Gross. Digital emotion contagion. *Trends in Cognitive Sciences*, 24(4):316–328, 2020.
- [19] Susannah BF Paletz, Michael A Johns, Egle E Murauskaite, Ewa M Golonka, Nick B Pandža, C Anton Rytting, Cody Buntain, and Devin Ellis. Emotional content and sharing on Facebook: A theory cage match. *Science Advances*, 9(39):eade9231, 2023.
- [20] Lara Schreurs and Laura Vandenbosch. Introducing the social media literacy (smile) model with the case of the positivity bias on social media. *Journal of Children and Media*, 15(3):320–337, 2021.
- [21] Pavica Sheldon and Katherine Bryant. Instagram: Motives for its use and relationship to narcissism and contextual age. *Computers in Human Behavior*, 58:89–97, 2016.
- [22] Erin L Spottswood and Jeffrey T Hancock. The positivity bias and prosocial deception on Facebook. *Computers in Human Behavior*, 65:252–259, 2016.
- [23] Paul Rozin and Edward B Royzman. Negativity bias, negativity dominance, and contagion. *Personality and Social Psychology Review*, 5(4):296–320, 2001.
- [24] Silvia Knobloch-Westerwick, Cornelia Mothes, and Nick Polavin. Confirmation bias, ingroup bias, and negativity bias in selective exposure to political information. *Communication Research*, 47(1):104–124, 2020.
- [25] Stuart Soroka, Patrick Fournier, and Lilach Nir. Cross-national evidence of a negativity bias in psychophysiological reactions to news. *Proceedings of the National Academy of Sciences*, 116(38):18888–18892, 2019.
- [26] Lorenzo Coviello, Yunkyu Sohn, Adam DI Kramer, Cameron Marlow, Massimo Franceschetti, Nicholas A Christakis, and James H Fowler. Detecting emotional contagion in massive social networks. *PloS One*, 9(3):e90315, 2014.
- [27] Anatoliy Gruzd, Sophie Doiron, and Philip Mai. Is happiness contagious online? A case of Twitter and the 2010 winter olympics. In *2011 44th Hawaii International Conference on System Sciences*, pages 1–9. IEEE, 2011.
- [28] Adam DI Kramer, Jamie E Guillory, and Jeffrey T Hancock. Experimental evidence of massive-scale emotional contagion through social networks. *Proceedings of the National Academy of Sciences of the United States of America*, 111(24):8788, 2014.
- [29] Rui Fan, Ke Xu, and Jichang Zhao. Higher contagion and weaker ties mean anger spreads faster than joy in social media. *arXiv preprint arXiv:1608.03656*, 2016.
- [30] Mufan Luo, Tiffany W Hsu, Joon Sung Park, and Jeffrey T Hancock. Emotional amplification during live-streaming: Evidence from comments during and after news events. *Proceedings of the ACM on Human-computer Interaction*, 4(CSCW1):1–19, 2020.
- [31] Didier Sornette. *Endogenous versus exogenous origins of crises*. in “Extreme Events in Nature and Society,” Series: The Frontiers Collection S. Albeverio, V. Jentsch and H. Kantz, eds. (Springer, Heidelberg, 2005 (<http://arxiv.org/abs/physics/0412026>)).
- [32] Alexander Saichev and Didier Sornette. Generating functions and stability study of multivariate self-excited epidemic processes. *The European Physical Journal B*, 83(2):271, 2011.
- [33] Alexander Saichev, Thomas Maillart, and Didier Sornette. Hierarchy of temporal responses of multivariate self-excited epidemic processes. *The European Physical Journal B*, 86:1–19, 2013.

- [34] Paul Ekman. An argument for basic emotions. *Cognition & Emotion*, 6(3-4):169–200, 1992.
- [35] Yinhan Liu, Myle Ott, Naman Goyal, Jingfei Du, Mandar Joshi, Danqi Chen, Omer Levy, Mike Lewis, Luke Zettlemoyer, and Veselin Stoyanov. Roberta: A robustly optimized Bert pretraining approach. *arXiv preprint arXiv:1907.11692*, 2019.
- [36] Eliska Prochazkova and Mariska E Kret. Connecting minds and sharing emotions through mimicry: A neurocognitive model of emotional contagion. *Neuroscience & Biobehavioral Reviews*, 80:99–114, 2017.
- [37] Patrick J Laub, Young Lee, and Thomas Taimre. *The elements of Hawkes processes*. Springer, 2021.
- [38] Shyam Nandan, Sumit Kumar Ram, Guy Ouillon, and Didier Sornette. Is seismicity operating at a critical point? *Physical Review Letters*, 126(12):128501, 2021.
- [39] Pierre Blanc, Jonathan Donier, and J-P Bouchaud. Quadratic Hawkes processes for financial prices. *Quantitative Finance*, 17(2):171–188, 2017.
- [40] Alexander Wehrli, Spencer Wheatley, and Didier Sornette. Scale-, time- and asset-dependence of Hawkes process estimates on high frequency price changes. *Quantitative Finance*, 21(5):729–752, 2021.
- [41] Riley Crane and Didier Sornette. Robust dynamic classes revealed by measuring the response function of a social system. *Proceedings of the National Academy of Sciences*, 105(41):15649–15653, 2008.
- [42] Ryota Kobayashi and Renaud Lambiotte. Tideh: Time-dependent Hawkes process for predicting retweet dynamics. In *Proceedings of the International AAAI Conference on Web and Social Media*, volume 10, pages 191–200, 2016.
- [43] Zorah Hilvert-Bruce, James T Neill, Max Sjöblom, and Juho Hamari. Social motivations of live-streaming viewer engagement on Twitch. *Computers in Human Behavior*, 84:58–67, 2018.
- [44] William A Hamilton, Oliver Garretson, and Andruid Kerne. Streaming on Twitch: Fostering participatory communities of play within live mixed media. In *Proceedings of the SIGCHI Conference on Human Factors in Computing Systems*, pages 1315–1324, 2014.
- [45] Jessica M Salerno and Liana C Peter-Hagene. The interactive effect of anger and disgust on moral outrage and judgments. *Psychological Science*, 24(10):2069–2078, 2013.
- [46] William J Brady, Killian L McLoughlin, Mark P Torres, Kara F Luo, Maria Gendron, and MJ Crockett. Overperception of moral outrage in online social networks inflates beliefs about intergroup hostility. *Nature Human Behaviour*, 7(6):917–927, 2023.
- [47] Ethan Kross, Philippe Verduyn, Gal Sheppes, Cory K Costello, John Jonides, and Oscar Ybarra. Social media and well-being: Pitfalls, progress, and next steps. *Trends in Cognitive Sciences*, 25(1):55–66, 2021.
- [48] John Suler. The online disinhibition effect. *Cyberpsychology & Behavior*, 7(3):321–326, 2004.
- [49] Madelyn R Sanfilippo, Pnina Fichman, and Shengnan Yang. Multidimensionality of online trolling behaviors. *The Information Society*, 34(1):27–39, 2018.
- [50] Justin Cheng, Michael Bernstein, Cristian Danescu-Niculescu-Mizil, and Jure Leskovec. Anyone can become a troll: Causes of trolling behavior in online discussions. In *Proceedings of the 2017 ACM Conference on Computer Supported Cooperative Work and Social Computing*, pages 1217–1230, 2017.
- [51] Empathic AI can’t get under the skin. *Nature Machine Intelligence*, 6(5):495–495, 2024. Editorial.



- [52] Xinzhi Wang, Luyao Kou, Vijayan Sugumaran, Xiangfeng Luo, and Hui Zhang. Emotion correlation mining through deep learning models on natural language text. *IEEE Transactions on Cybernetics*, 51(9):4400–4413, 2020.
- [53] Peng Xu, Zihan Liu, Genta Indra Winata, Zhaojiang Lin, and Pascale Fung. Emograph: Capturing emotion correlations using graph networks. *arXiv preprint arXiv:2008.09378*, 2020.
- [54] Saif Mohammad, Felipe Bravo-Marquez, Mohammad Salameh, and Svetlana Kiritchenko. Semeval-2018 task 1: Affect in tweets. In *Proceedings of the 12th International Workshop on Semantic Evaluation*, pages 1–17, 2018.
- [55] Spencer Wheatley, Alexander Wehrli, and Didier Sornette. The endo–exo problem in high frequency financial price fluctuations and rejecting criticality. *Quantitative Finance*, 19(7):1165–1178, 2019.
- [56] Thijs Pollmann. On forgetting the historical past. *Memory & Cognition*, 26:320–329, 1998.
- [57] Didier Sornette. *Critical Phenomena in Natural Sciences: Chaos, Fractals, Selforganization and Disorder: Concepts and Tools*. Springer Science & Business Media, 2006.
- [58] Vladimir Filimonov and Didier Sornette. Apparent criticality and calibration issues in the hawkes self-excited point process model: Application to high-frequency financial data. *Quantitative Finance*, 15:1293–1314, 2015.
- [59] Vladimir Filimonov and Didier Sornette. Quantifying reflexivity in financial markets: Toward a prediction of flash crashes. *Physical Review E*, 85(5):056108, 2012.
- [60] Stephen J Hardiman, Nicolas Bercot, and Jean-Philippe Bouchaud. Critical reflexivity in financial markets: A Hawkes process analysis. *The European Physical Journal B*, 86:1–9, 2013.
- [61] Shyam Nandan, Guy Ouillon, and Didier Sornette. Are large earthquakes preferentially triggered by other large events? *Journal of Geophysical Research: Solid Earth*, 127(8):e2022JB024380, 2022.
- [62] Jiawei Li, Didier Sornette, Zhongliang Wu, Jiancang Zhuang, and Changsheng Jiang. Revisiting seismicity criticality: A new framework for bias correction of statistical seismology model calibrations. *arXiv preprint arXiv:2404.16374*, 2024.
- [63] Benjamin B Machta, Ricky Chachra, Mark K Transtrum, and James P Sethna. Parameter space compression underlies emergent theories and predictive models. *Science*, 342(6158):604–607, 2013.

# SI Appendix

## A Summary Statistics of YouTube Live Chat Data

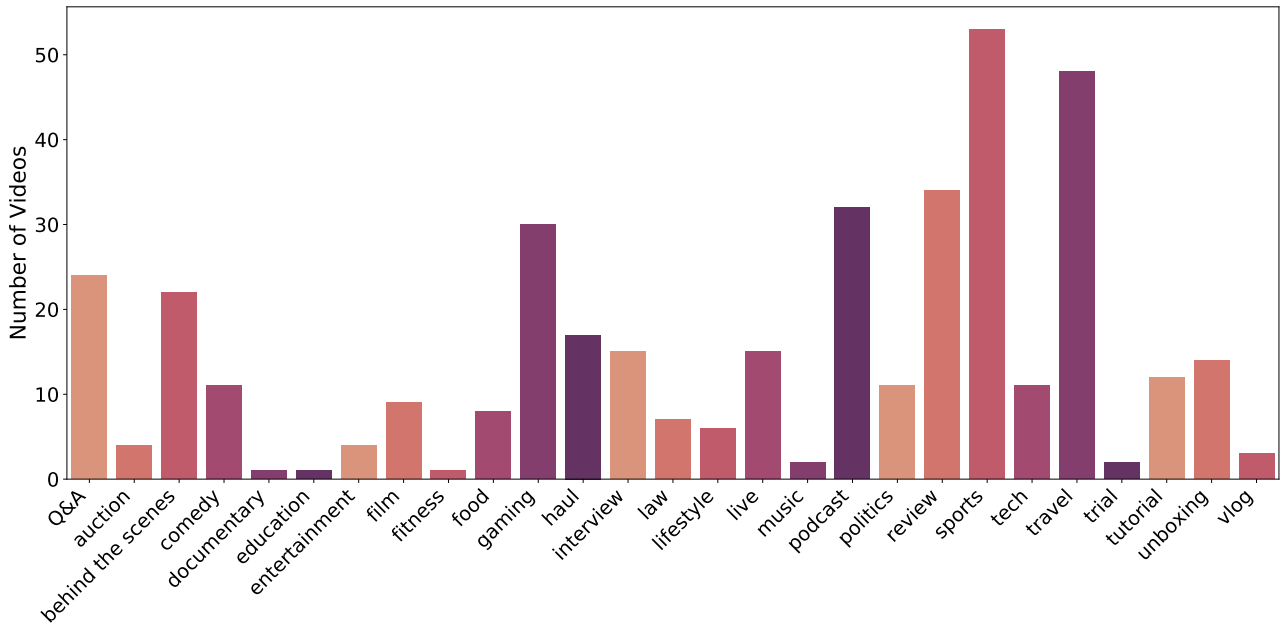


Figure A.1: Number of videos per keyword in our final data sample across 27 keywords.

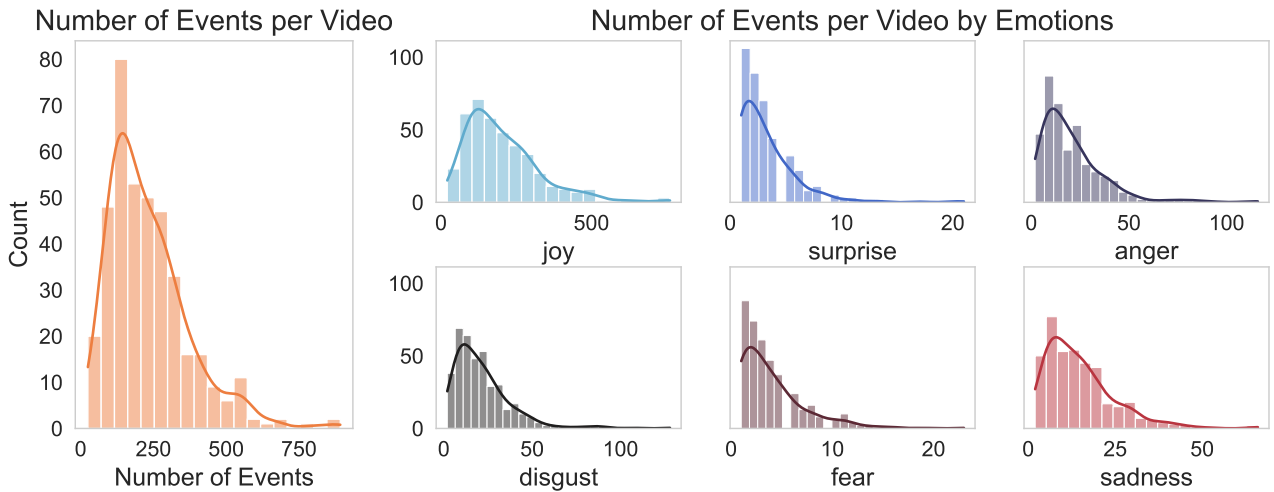


Figure A.2: (left) Distribution of the number of events per video across 397 videos. (right) Same as left but broken down per emotion.

We show some additional summary statistics of our dataset. The final sample of our data contains 92,412 live chat messages across 397 videos, adding up to 780 hours of content and covering 27 topics. The distribution of topics is shown in Figure A.1. The distribution of emotional events is shown in Figure A.2. We also show the distribution of the median time between each event arrival in Figure A.3. Since we label emotions non-exclusively, we show the co-occurrence patterns across 6 basic emotions in Figure A.4. In general, negative emotions have a higher tendency to co-occur with one another. In particular, anger and disgust have a relatively high co-occurrence.

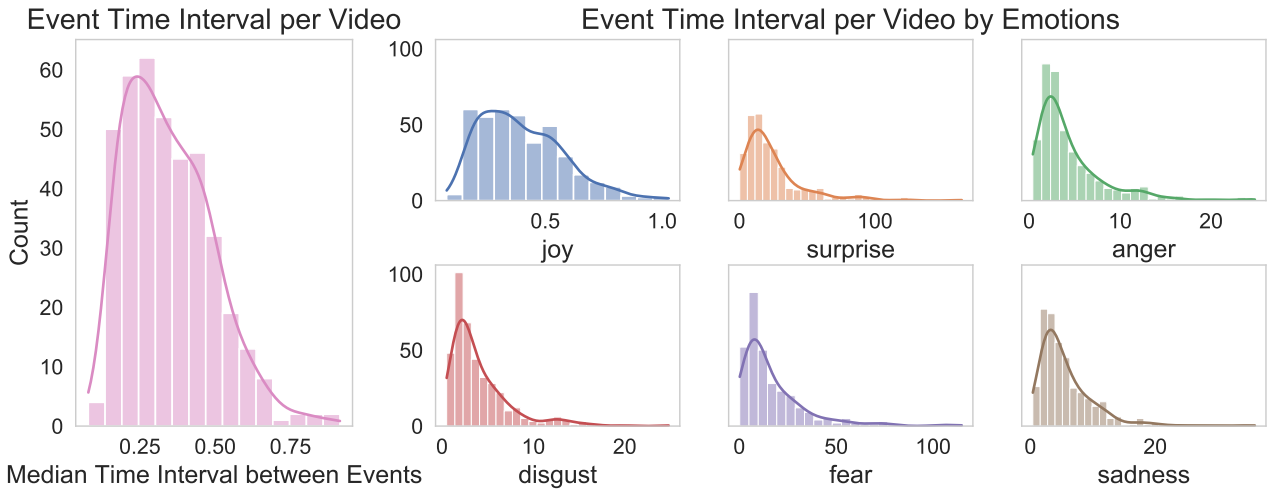


Figure A.3: (left) Distribution of the median time interval between each event in units of minutes for each video across 397 videos. (right) Same as left but broken down per emotion.

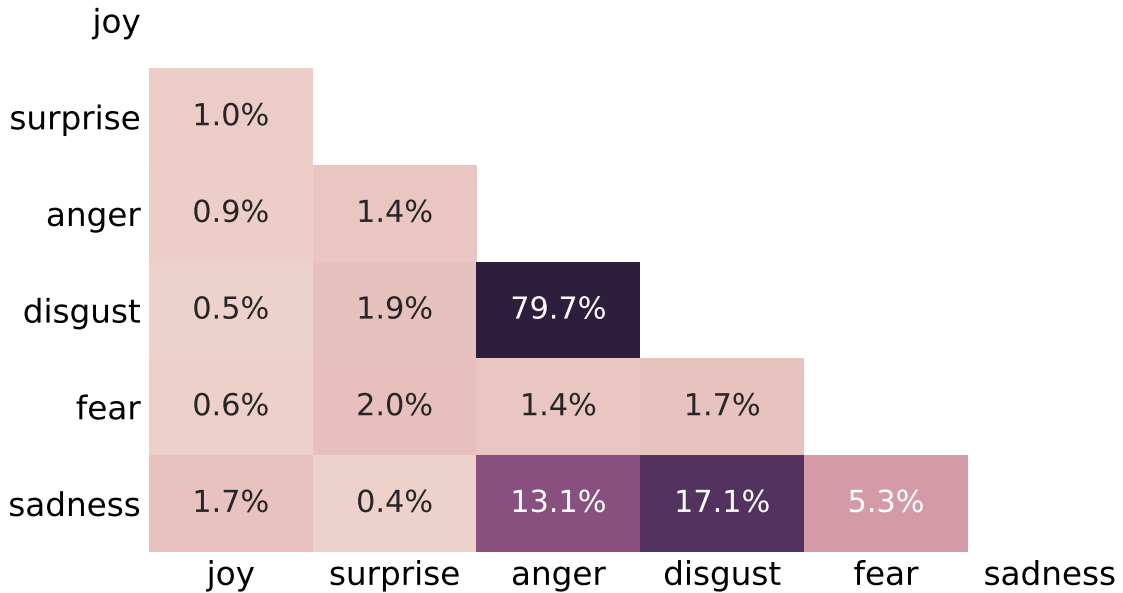
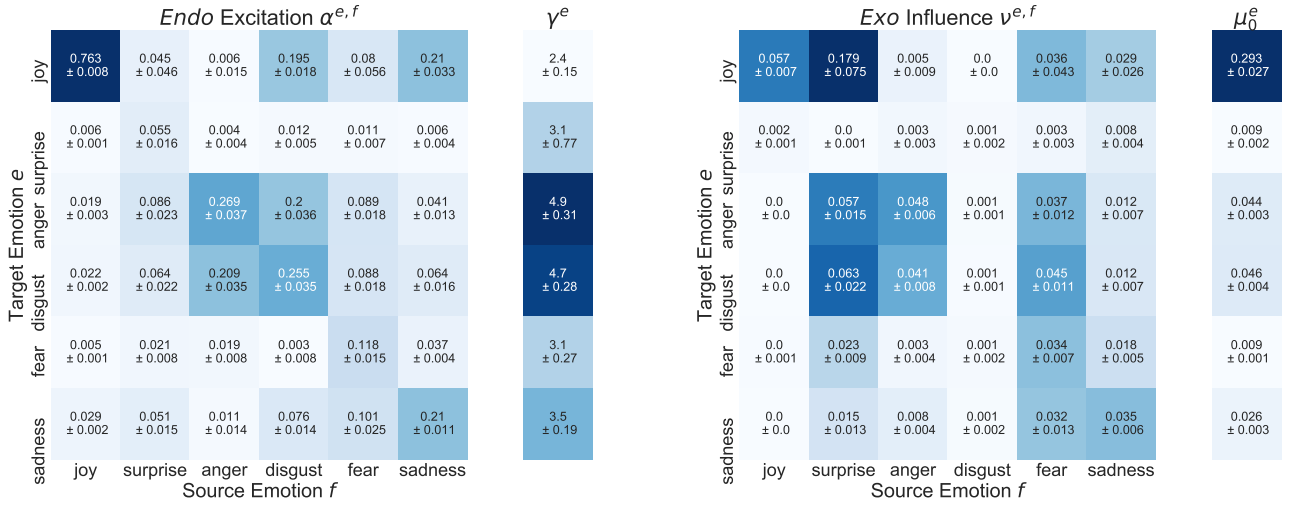


Figure A.4: Co-occurrence of emotions in our data. We normalize the number of co-occurrences for each emotion pair by the sum of occurrences of the two emotions in the live chat.

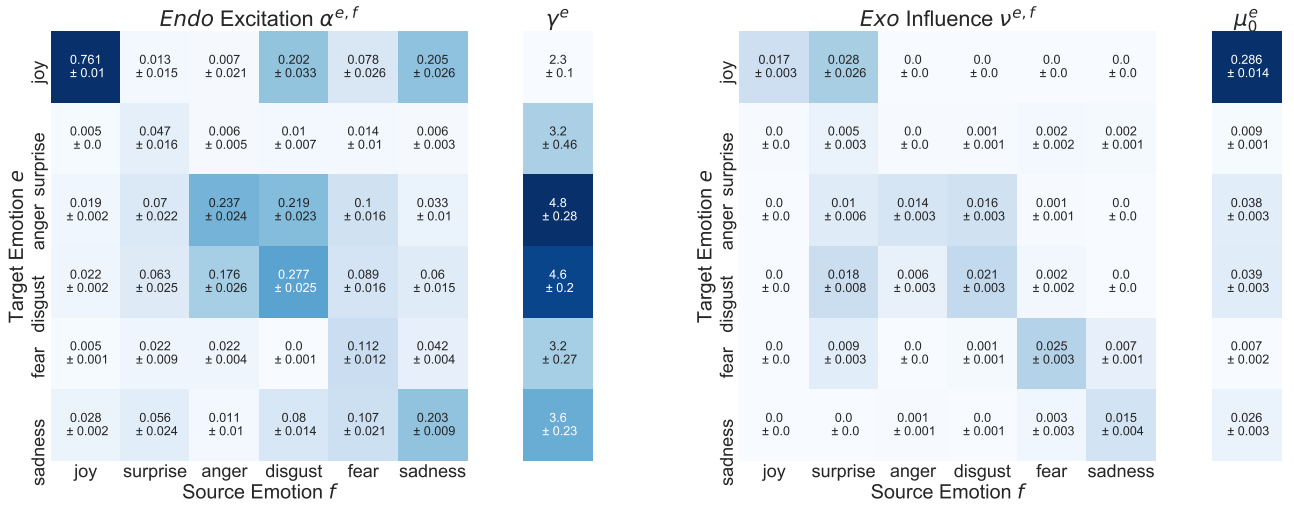
## B Robustness Analysis on Video Influence

To examine the impact of video content on live chat discussions, we have parameterized and interpolated the prevalence of emotions in the video via sums of log-normal shapes (see Methods). Here, we test the robustness of our results with respect to changes in the log-normal parameters. We have defined the log-normal function with 2 parameters, the maximum, and the median. We assumed that the intensity of each transcript peaks 2 seconds after appearance such that the maximum of the log-normal function lies at 2 seconds. We further assumed that 50% of the emotion intensity for each transcript is manifested within 10 seconds of transcript appearance such that the median is equal to 10 seconds. Here we repeat our analysis while changing the log-normal function maximum and median by factors of 0.5 and 2 to test the robustness of our results. This effectively changes assumptions about the audience’s reaction time and memory of prior content. We observe in Figures B.1a, B.1b, B.2a, and B.2b that the results with the different log-normal parameters are highly consistent with our results in the main text.

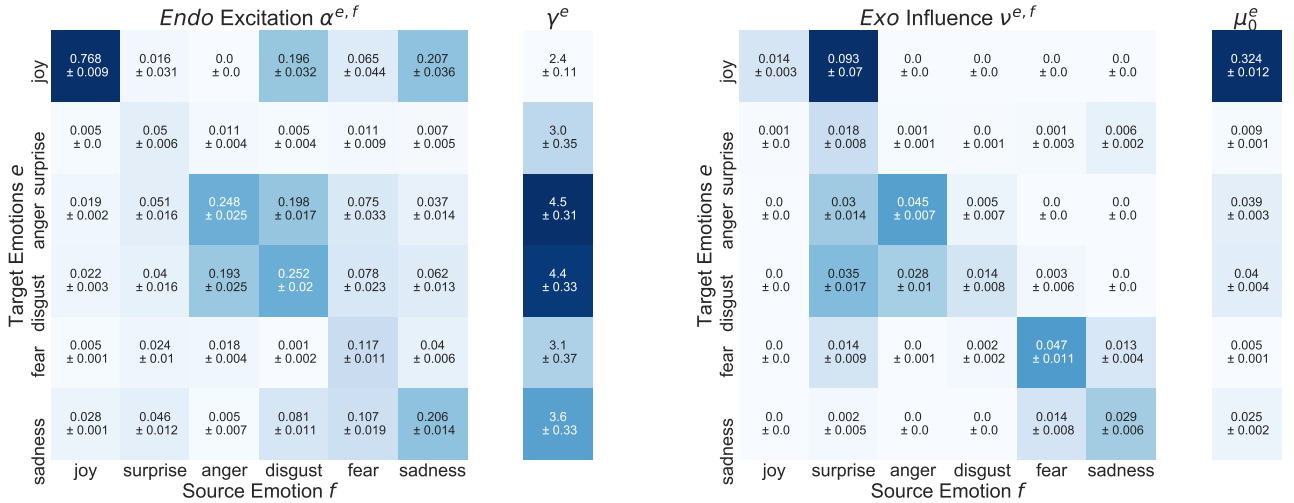
Human memory decays following an approximate power law [56]. The log-normal function resembles the shape of a power law over a limited range of the variable, which is all the larger, the larger is  $\sigma$  [57]. We thus test our results with an alternative parametrization of the video influence in a power law shape where  $s_{\tau_j}^f(t) = \frac{1}{(t-\tau_j)^c}$ . We show examples in Figure B.1c and B.2c for  $c = 2.5$ , and find that the results are qualitatively consistent with the results we obtain from the log-normal over a range of  $c$  values from 2.5 to 10.



(a)



(b)



(c)

Figure B.1: To test the validity of our video parametrization method, we repeat the analysis while changing the parameters of the video influence function as well as the influence function shape. This Figure shows the estimated parameters of our log-likelihood function in Equation (5) in the main text. Figures B.1a and B.1b show the estimated parameters when multiplying the maximum and median in the log-normal function by a factor of 0.5 and 2, respectively. Figure B.1c shows the estimated parameters when parametrizing the video influence with a power law shape. The estimated parameters are highly consistent with our main result (Figure 2 in the main text).



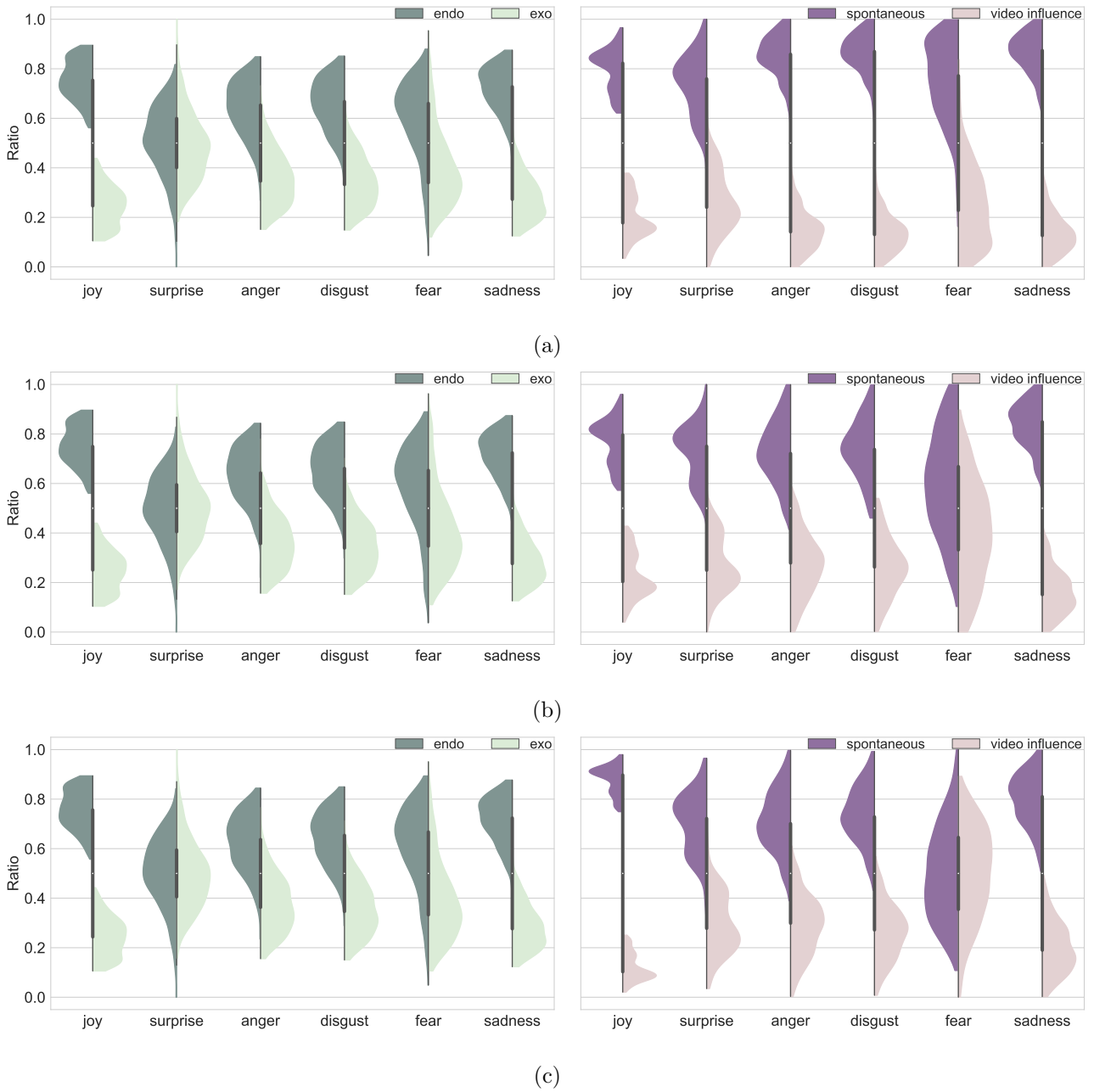


Figure B.2: Figures B.1a and B.1b show the relative source of influence when multiplying the maximum and median in the log-normal function by a factor of 0.5 and 2, respectively. Figure B.1c shows the relative source of influence when parametrizing the video influence with a power law shape. The left column shows the relative percentage of endogenous and exogenous influence. The right column zooms in on the exogenous influence and examines the relative source of mother events from spontaneous user expressions and video influence. The relative influences are highly consistent with our main result (Figure 3 in the main text). The endogenous influence is comparably larger than the exogenous influence, and the source of mother events is predominately spontaneous user expressions.

## C Dynamics of 4 Emotions

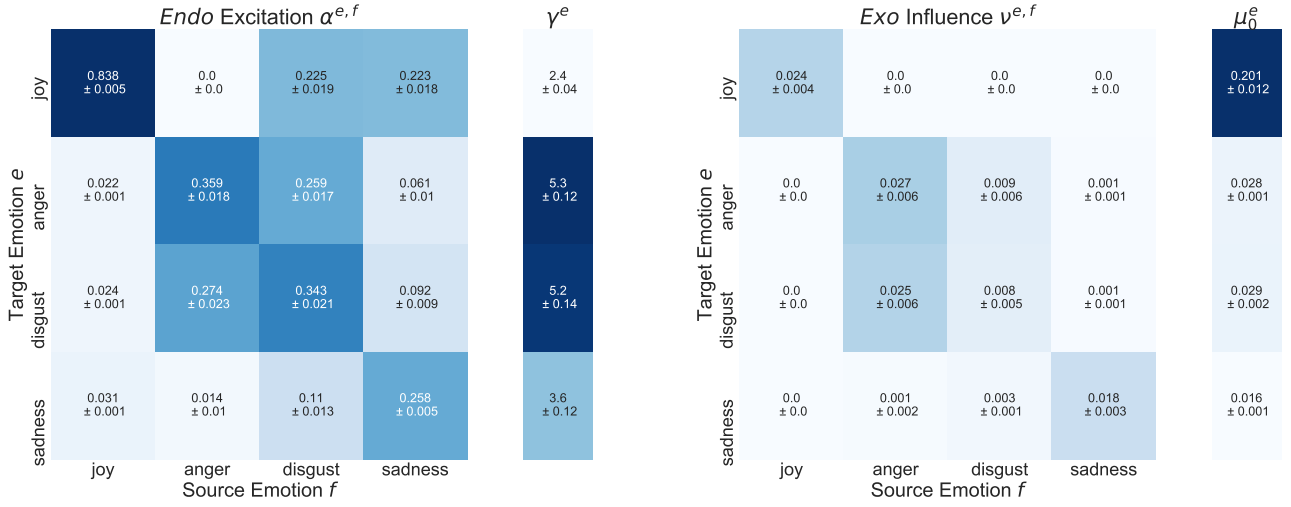


Figure C.1: This figure shows the estimated parameters of our log-likelihood function in Equation (5) in the main text for 4 emotions. The estimations are consistent with our main results (Figure 2 in the main text).



Figure C.2: This left plot shows the relative ratios of endogenous and exogenous influences. The right plot shows the ratios of mother events from spontaneous expression and video influence. We observe that the endogenous influence dominates the emotion dynamics in YouTube live chats. In addition, the mother events mostly stem from spontaneous user expressions rather than video influence. This is consistent with our main result (Figure 3 in the main text).

Our main analysis models the commonly studied 6 basic emotions [34]. Here we test the robustness of our results by modeling  $|\mathcal{E}| = 4$  emotions: joy, anger, disgust, and sadness, removing *fear* and *surprise* because they have small excitatory patterns and low overall intensity. We obtain a sample of 288,581 live chat messages across 1,405 videos. Reducing the dimensionality of the multivariate Hawkes process reduces the number of parameters to be estimated  $|\mathcal{E}|(2|\mathcal{E}| + 2)$  from 84 to 40.

We obtain our results for 4 emotions in Figures C.1 and C.2. We find that the dynamics of 4 emotions are qualitatively similar to our main results on 6 emotions (Figures 2 and 3 in the main text).

## D Sub-sample Analysis with Different Video Types

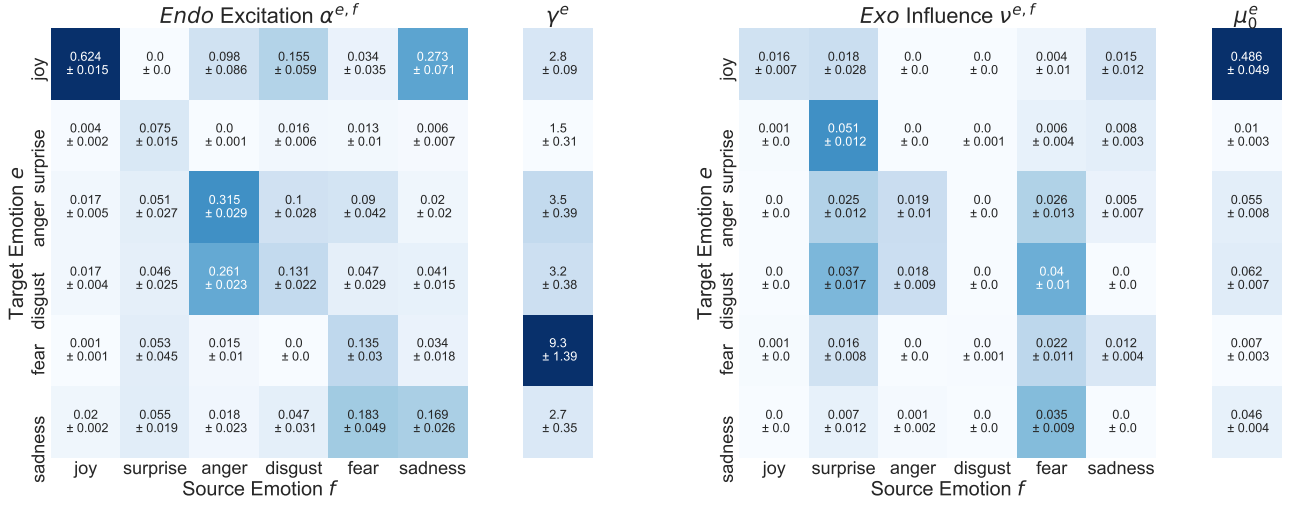


Figure D.1: This figure shows the estimated parameters of our log-likelihood function in Equation (5) in the main text for sports videos. The estimations are largely consistent with our main result (Figure 2 in the main text).

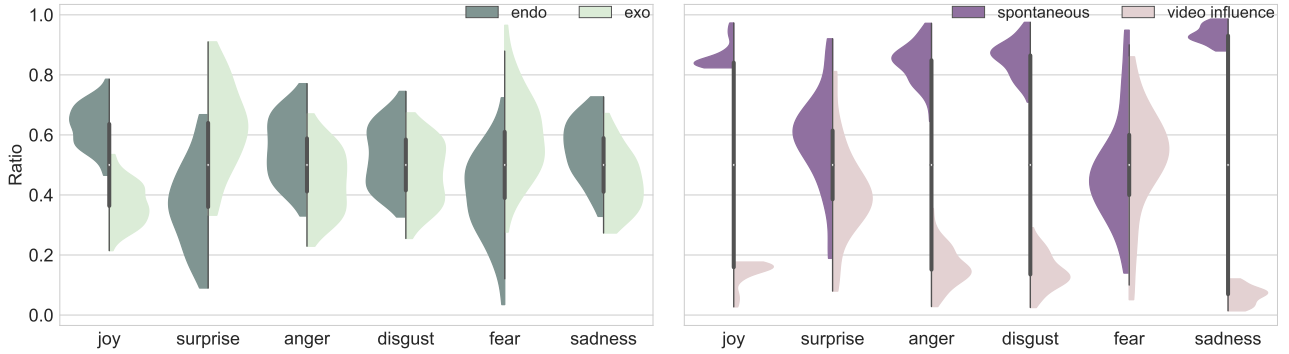


Figure D.2: This left plot shows the relative ratios of endogenous and exogenous influences for sports videos. The right plot shows the ratios of mother events from spontaneous expression and video influence for sports videos. We observe that the exogenous influence has a larger impact on emotion intensities for sports videos compared to our main result (Figure 3 in the main text). In particular, the emotions of surprise and fear are largely exogenously driven. The mother events are induced more by spontaneous expressions rather than video influence.

Our main analysis examines general emotional and behavioral patterns among online users by compiling 92,412 YouTube live chat messages across 27 topics. Yet the susceptibility of emotion dynamics to video influence and peer interactions is potentially subject to the type of video and the audience community. Here, we conduct sub-sample analyses on representative video types to identify heterogeneity in the evolution of online emotion dynamics. First, we focus on live sports videos with a total of 11,172 live chat messages. Figures D.1 and D.2 show estimated parameters and relative sources of influence for live sports shows. We identify similarities to our results in the main text. The emotion of joy is the most contagious. Anger tends to self-excite and trigger disgust. Given the natural conflict from sports competitions, we observe cross-triggering between sadness and joy. In particular, users have a much longer direct memory of fear than other emotion types. Users have a much higher propensity for joyful expression which coincides with the entertaining nature of sports events. However, compared to our main result (Figure 3 in the main text), the emotion dynamics are more susceptible to exogenous influences. In particular, the emotions of surprise and fear are the most exogenously driven.

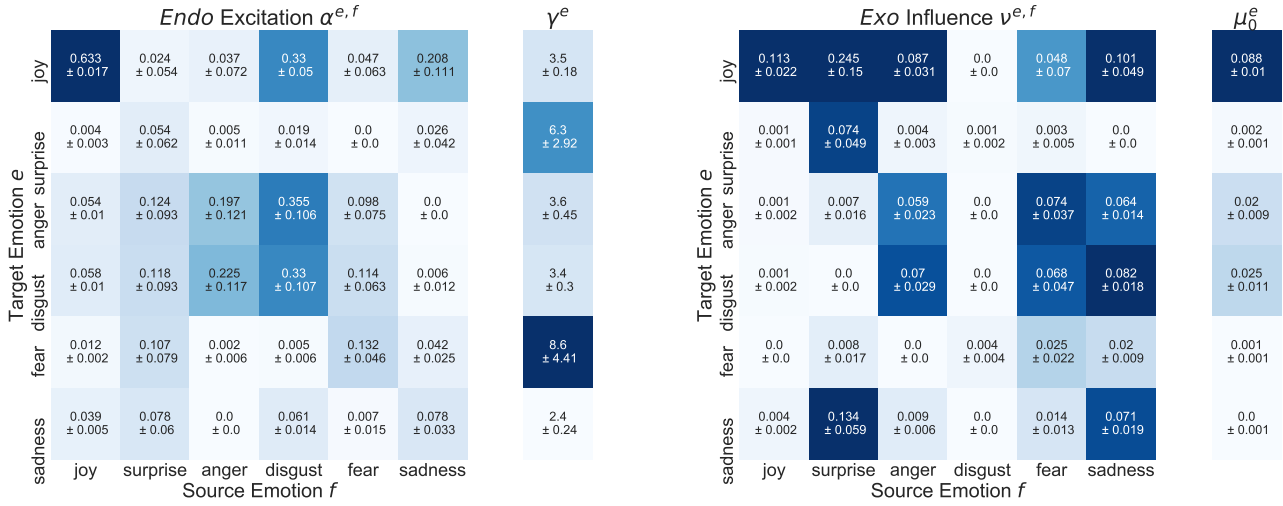


Figure D.3: This figure shows the estimated parameters of our log-likelihood function in Equation (5) in the main text for political videos. We observe that joy remains the most contagious emotion, and the cross-triggering effects between anger and disgust are prominent in the political context. The emotions of surprise and fear impose significantly longer direct memories on users.

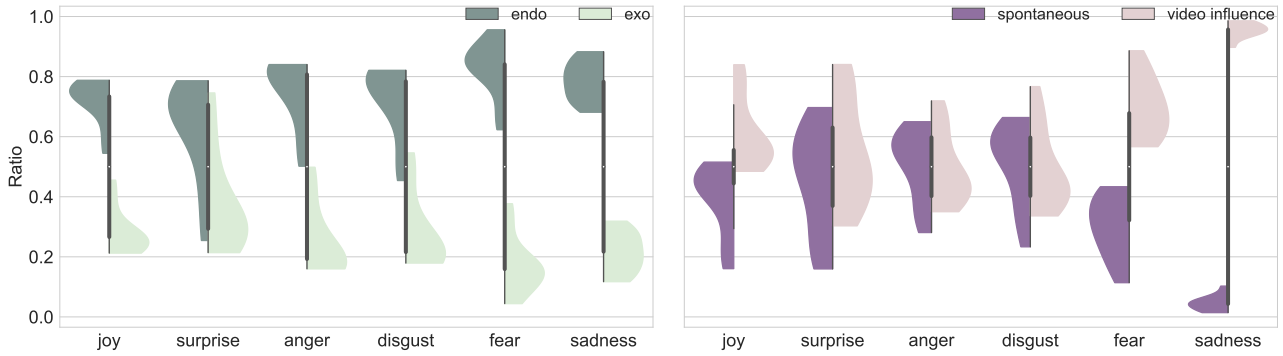


Figure D.4: This left plot shows the relative ratios of endogenous and exogenous influences for political videos. The right plot shows the ratios of mother events from spontaneous expression and video influence for political videos. We observe that endogenous influence strongly dominates the emotion dynamics in political discussions. As opposed to our main result in (Figure 3 in the main text), political videos are more stimulative of discussions than the average video content.

Second, we study political videos with a total of 3,043 live chat messages to understand how emotions evolve in political discussions. We highlight the cross-triggering of anger and disgust which contributes to moral outrage commonly observed in the political context. Users have longer-lasting direct memories of fear and surprise in online discussions. Political content is often accompanied by contentious discussions. In fact, we observe that endogenous interactions dominate exogenous influence by a large margin across emotion types. However, different from our main result (Figure 3 in the main text), the video content has a comparatively larger influence than spontaneous expressions in driving the emotion dynamics. This shows that political videos are highly stimulative in evoking emotional reactions in the audience. We observe that heterogeneity in online emotion evolution can arise from differences in video content and audience characteristics.

## E Dynamics of Live Chats with No Emotional Content

Parameters:	$\alpha$	$\gamma$	$\mu$	$\nu$
Mean	0.857	1.967	0.150	0.029
Standard Deviation	0.018	0.167	0.022	0.006

Table 2: The mean and standard deviation of estimated parameters for a univariate Hawkes Process of live chat messages with no emotion labels across 10 bootstrapped samples.

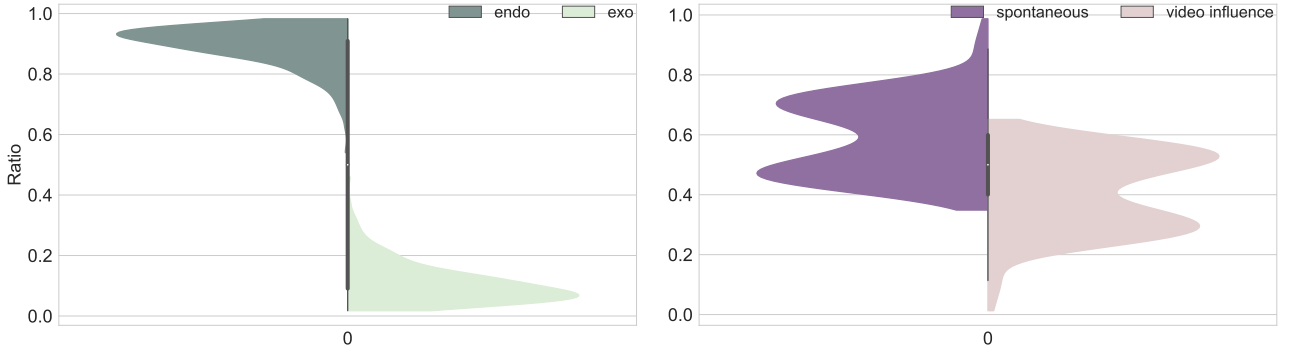


Figure E.1: The left plot shows the relative ratios of endogenous and exogenous influences for live chat messages with no emotion labels. The right plot shows the ratios of mother events from spontaneous expression and video influence for live chat messages with no emotion labels. We observe that the endogenous influence nonetheless dominates the dynamics of live chat messages with no emotion labels. However, the source of mother events is distributed more evenly between spontaneous expressions and video influence.

Our main study shows that online emotions are characterized by excitatory patterns. Despite the constant feed of video content, the emotion dynamics evolve mostly spontaneously among users. To complement our analysis, we study the behavior of live chats with no emotional content. We train a transformer to assign emotion labels for live chats. We deem the live chat messages that were not assigned any emotion labels as containing no emotional content. This gives us 66,235 live chat messages with no emotional content across 232 videos. We use a univariate Hawkes process to describe the intensity of live chat messages with no emotion labels. The intensity  $\lambda(t)$  at time  $t$  during a given video is specified as

$$\lambda(t) = \underbrace{\mu_0}_{\text{exo base rate}} + \underbrace{\nu S(t)}_{\text{exo video influence}} + \underbrace{\sum_{t_j < t} \phi(t - t_j)}_{\text{endo chat influence}}. \quad (1)$$

The value of  $S(t)$  is given by  $S(t) = \sum_{\tau_j < t} s_{\tau_j}(t)$  where  $\{\tau_j\}$  enumerates all times at which a subtitle first appears in the video. The values of  $s_{\tau_j}(t)$  are computed according to Equation (3) from the main text with  $\mu = 2.3$  and  $\sigma = 1.3$ . The term  $s_{\tau_j}(t)$  represents the time-varying intensity arising from a video subscript appearing in the video at time  $\tau_j$ . Similarity, we assume that  $\phi$  is exponentially decaying where  $\phi(t) = \alpha \frac{1}{\gamma} e^{-\frac{1}{\gamma}t}$  with decay time  $\gamma$ . Table 2 shows the estimated parameters of Equation (1). We observe that live chat messages with no emotional content are nonetheless highly self-exciting, but with a shorter direct memory than emotional live chats. Different from our main result (Figure 3 in the main text), live chat messages with no emotional content are driven more equally by the video and user spontaneity as shown in Figure E.1. This shows that while live discussions largely evolve endogenously, live chats with no emotional content are much more affected by the videos. In contrast, emotions on online platforms are largely attributed to user expressions and interactions.



## F Baseline Intensity Calibration in Hawkes Process

Correctly calibrating the baseline intensity is crucial to the reliability of Hawkes process estimations. Insights from the field of finance illustrate how non-constant background intensity can bias the branching ratio estimation [58, 55, 40]. There has been a debate over whether financial markets are operating at criticality. Calibration of the Hawkes model on financial time series had shown that the branching ratio is less than 1, thus rejecting criticality [59]. Subsequently, alternative estimation reported a branching ratio close to 1, suggesting that markets are operating at criticality [60]. Both studies obtained their results from the calibration of a temporal Hawkes model assuming constant baseline intensity. The opposing findings have to do with the length of the financial time series and the non-stationarity. Specifically, the latter study used time series of long durations over multiple months [60]. In contrast, the former study rejecting criticality used much shorter time series from 10 to 30 minutes due to the concern of non-stationarity of longer time series [59]. As shown by subsequent studies, financial time series are in fact temporally non-stationary, being highly volatile at market openings and closings, and stable around lunch hours [55, 40]. As a result, calibrating the Hawkes model with time series over multiple days with the erroneous assumption of constant baseline intensity will artificially inflate the branching ratio towards 1 to account for the non-stationarity omitted in the background. Using an advanced Hawkes model calibration that employs the expectation-maximization (EM) method to parameterize non-constant baseline intensity over financial time series spanning several months, the hypothesis of market criticality is rejected [55, 40].

In the field of earthquake prediction, advanced Epidemic-Type Aftershock Sequences (ETAS) (also known as Hawkes model in the domain of finance and mathematics) calibration has been proposed which features a superior parametric representation of the spatially varying background seismicity rate [38, 61]. A recent study further improves the methodology to avoid biases in the estimation of the branching ratio [62]. Studies have shown that the branching ratio of earthquake activities for the global, California, New Zealand, and Sichuan and Yunnan provinces in China are below 1, revealing sub-critical seismicity [38, 61, 62]. However, it has been shown that constraining to a constant baseline intensity results in the false conclusion that the branching ratio approaches 1, suggesting seismicity criticality [38, 61, 62]. Assuming a constant baseline intensity in the ETAS estimation neglects the spatial heterogeneity of the background seismicity. Consequently, the branching ratio is biased towards 1 where the perceived criticality is a statistical artifact arising from the incorrectly specified ETAS model attempting to account for the activities in the background seismicity.

In conclusion, it is essential to allow for non-stationarity and non-uniformity of the baseline intensity in order to avoid several biases in the parameter estimation of the Hawkes process, and in particular in the determination of its branching ratio.

## G Log-Likelihood Derivation

We define a general multivariate Hawkes self-excited conditional point process [32, 33] as follows. We observe  $|\mathcal{E}|$  point processes. For each process  $e \in \mathcal{E}$ , we observe  $N^e$  events,  $i = 1, \dots, N^e$ , where event  $i$  of process  $e$  takes place at time point  $t_i^e$ ,  $i = 1, \dots, N^e$ . We define  $t_0^e \equiv 0$ ,  $t_{N^e+1}^e \equiv T$  for  $e \in \mathcal{E}$ , such that the observation period over the entire process is  $\{t_i^e \mid i^e = 0, \dots, N^e + 1\}$ . We denote the intensity at time  $t$  for a given process as

$$\lambda^e(t) = \mu^e(t) + \sum_{f \in \mathcal{E}} \sum_{t_j^f < t} \phi^{e,f}(t - t_j^f), \quad (1)$$

where  $t_j^f$  enumerates all past events of process  $f$  that took place before  $t$ . The function  $\phi^{e,f}(t)$  is defined to only take positive values. The term  $\mu^e(t)$  represents the exogenous component of the Hawkes process leading to spontaneous occurrence of events, whereas  $\sum_{f \in \mathcal{E}} \sum_{t_j^f < t} \phi^{e,f}(t - t_j^f)$  represents the endogenous impact from past events in process  $f$  on process  $e$ . In the current form, we can estimate all parameters for fixed  $e$ .

We derive the log-likelihood function for a fairly general class of the Hawkes process as follows. The expected number of events for emotion  $e$  within time interval  $\Delta t$  is approximately  $\lambda^e(t)\Delta t$  for small  $\Delta t$ 's. In the limit of an infinitesimally small time interval  $\Delta t \rightarrow dt$ , the term  $\lambda^e(t)dt$  then represents the probability of observing exactly one event, since the probability of observing more than one event is an infinitesimal of higher order (technically proportional to  $dt^2$ ). Similarly, the probability of not observing any event within  $dt$  reads  $1 - \lambda^e(t)dt$ , which, in the limit of  $dt$  infinitesimal, becomes equivalent to  $\exp(-\lambda^e(t)dt)$ . The probability of not observing any event over a finite time  $\Delta t$  is thus  $\exp\left(-\int_t^{t+\Delta t} d\tau \lambda^e(\tau)\right)$  by the law of independent probabilities. Taken together, the likelihood function capturing event intensity at  $t_i$  over  $[0, T]$  reads

$$\prod_{i=1}^{N^e} \lambda^e(t_i) e^{-\int_{t_i}^{t_{i+1}} ds \lambda^e(s)}. \quad (2)$$

Taking the product over the exponential terms, Equation (2) simplifies to  $\prod_{i=1}^{N^e} \lambda^e(t_i) e^{-\int_0^T ds \lambda^e(s)}$ . The Hawkes process likelihood function is thus

$$L^e(\rho^e, \theta^{e,f}) = \prod_{i=1}^{N^e} \lambda^e(t_i) e^{-\int_0^T ds \lambda^e(s)}. \quad (3)$$

The log-likelihood function of a general multivariate Hawkes process is thus

$$\log(L^e(\theta^{e,f})) = \sum_{i=1}^{N^e} \log(\lambda^e(t_i)) - \int_0^T ds \lambda^e(s) \quad (4a)$$

$$= \sum_{i=1}^{N^e} \log(\lambda^e(t_i)) - \int_0^T ds \mu^e(s) - \sum_{f \in \mathcal{E}} \sum_{t_j^f} \int_{t_j^f}^T ds \phi^{e,f}(s). \quad (4b)$$

It is common to assume  $\phi^{e,f}(t) = \alpha^{e,f} \frac{1}{\gamma^e} e^{-\frac{1}{\gamma^e} t}$ . For simplicity and as a way to address the fact that the parameter  $\gamma^e$  is ‘‘sloppy’’, which means that the log-likelihood function has a very large radius of curvature close its maximum along the  $\gamma^e$  dimension, we assume  $\gamma^e$  to be constant across all processes.

Expanding Equation (4b), the log-likelihood function is written as

$$\log L^e(\alpha^{e,f}, \gamma^e) \stackrel{(4b)}{=} \sum_{i=1}^{N^e} \log(\lambda^e(t_i)) - \int_0^T ds \mu^e(s) - \sum_{f \in \mathcal{E}} \sum_{t_j^f} \int_{t_j^f}^T ds \alpha^{e,f} \frac{1}{\gamma^e} e^{-\frac{1}{\gamma^e}(s-t_j^f)} \quad (5a)$$

$$= \sum_{i=1}^{N^e} \log(\lambda^e(t_i)) - \int_0^T ds \mu^e(s) + \sum_{f \in \mathcal{E}} \sum_{t_j^f} \alpha^{e,f} e^{-\frac{1}{\gamma^e}(s-t_j^f)} \Big|_{t_j^f}^T \quad (5b)$$

$$= \sum_{i=1}^{N^e} \log \left( \mu^e(t_i) + \sum_{f \in \mathcal{E}} \sum_{t_j^f < t} \alpha^{e,f} \frac{1}{\gamma^e} e^{-\frac{1}{\gamma^e}(t_i-t_j^f)} \right) - \int_0^T ds \mu^e(s) + \sum_{f \in \mathcal{E}} \sum_{t_j^f} \alpha^{e,f} \left( e^{-\frac{1}{\gamma^e}(T-t_j^f)} - 1 \right). \quad (5c)$$

The following sections involve variations of the baseline intensity function, whereas the endogenous cross-excitation component is unchanged. We thus define  $\sum_{f \in \mathcal{E}} \sum_{t_j^f} \alpha^{e,f} \left( e^{-\frac{1}{\gamma^e}(T-t_j^f)} - 1 \right)$  from Equation (5c) as *endo* for the following derivation.

In our model, we allow for a coefficient term  $\nu^{e,f}$  which scales the effect of emotion  $f$  displayed in the video on emotion  $e$  in the chat. Concretely, we model the cross-excitation effects of the baseline function for process  $f$  on process  $e$ , namely  $\mu^e(t) = \mu_0^e + \mu_1^e(t) \equiv \mu_0^e + \sum_{f \in \mathcal{E}} \nu^{e,f} S^f(t)$ . We thus denote a multivariate Hawkes process for a given process as

$$\lambda^e(t) = \mu_0^e + \sum_{f \in \mathcal{E}} \nu^{e,f} S^f(t) + \sum_{f \in \mathcal{E}} \sum_{t_j^f < t} \phi^{e,f}(t - t_j^f) \quad (6)$$

where  $S^f(t)$  is known. The log-likelihood function is thus

$$\log(L^e(\mu_0^e, \nu^{e,f}, \theta^{e,f})) = \sum_{i=1}^{N^e} \log(\lambda^e(t_i)) - \int_0^T ds \lambda^e(s) \quad (7a)$$

$$= \sum_{i=1}^{N^e} \log(\lambda^e(t_i)) - \int_0^T ds \mu_0^e - \sum_{f \in \mathcal{E}} \nu^{e,f} \int_0^T ds S^f(s) - \sum_{f \in \mathcal{E}} \sum_{t_j^f} \int_{t_j^f}^T ds \phi^{e,f}(s). \quad (7b)$$

We assume  $\phi^{e,f}(t) = \alpha^{e,f} \frac{1}{\gamma^e} e^{-\frac{1}{\gamma^e}t}$ . Expanding Equation (7b), the log-likelihood function is written as

$$\log L^e(\mu_0^e, \nu^{e,f}, \alpha^{e,f}, \gamma^e) \stackrel{(7b)}{=} \sum_{i=1}^{N^e} \log(\lambda^e(t_i)) - \int_0^T ds \mu_0^e - \sum_{f \in \mathcal{E}} \nu^{e,f} \int_0^T ds S^f(s) + \text{endo} \quad (8a)$$

$$= \sum_{i=1}^{N^e} \log(\lambda^e(t_i)) - \int_0^T ds \mu_0^e - \sum_{f \in \mathcal{E}} \nu^{e,f} \int_0^T ds S^f(s) + \text{endo} \quad (8b)$$

$$= \sum_{i=1}^{N^e} \log \left( \mu_0^e + \sum_{f \in \mathcal{E}} \nu^{e,f} S^f(t) + \sum_{f \in \mathcal{E}} \sum_{t_j^f < t} \alpha^{e,f} \frac{1}{\gamma^e} e^{-\frac{1}{\gamma^e}(t-t_j^f)} \right) - \int_0^T ds \mu_0^e - \sum_{f \in \mathcal{E}} \nu^{e,f} \int_0^T ds S^f(s) + \text{endo} \quad (8c)$$

We compute  $\int_0^T ds S^f(s)$  numerically as  $M_1^f$ . Without loss of generality, we simplify the log-likelihood function to

$$\begin{aligned} \log L^e(\mu_0^e, \nu^{e,f}, \alpha^{e,f}, \gamma^e) &= \sum_{i=1}^{N^e} \log \left( \mu_0^e + \sum_{f \in \mathcal{E}} \nu^{e,f} S^f(t_i) + \sum_{f \in \mathcal{E}} \sum_{t_j^f < t} \alpha^{e,f} \frac{1}{\gamma^e} e^{-\frac{1}{\gamma^e}(t_i - t_j^f)} \right) - \\ &\mu_0^e T - \sum_{f \in \mathcal{E}} \nu^{e,f} M_1^f + \sum_{f \in \mathcal{E}} \sum_{t_j^f} \alpha^{e,f} \left( e^{-\frac{1}{\gamma^e}(T - t_j^f)} - 1 \right). \end{aligned} \quad (9)$$

## H Testing Log-Likelihood Fits with Synthetic Data

We estimate parameter values that maximize the log-likelihood function (9) via Quasi-Newton optimization. Without loss of generality, we normalize the log-likelihood function by the number of events  $N^e$ , in order to compare the log-likelihood values across different sample sizes. We use the Python ticks library <sup>4</sup> to simulate Hawkes processes with parameters that we refer to as the ground-truth. Subsequently, we compare the estimated parameters with their ground-truth values to evaluate performance. Since the parameters for each emotion are estimated separately, without loss of generality, we only show the synthetic test results for one emotion (process). The other processes have comparable performances. To assess the robustness of the estimation, we bootstrap the data and repeat the estimation 100 times.

The inset plots of Figure H.1 shows the distributions of estimated  $\mu_0^1$ ,  $\gamma^1$ ,  $\alpha^{1,f}$ , and  $\nu^{1,f}$  values for 100 bootstrap samples with  $N^e$  around 10,000. The dashed red lines mark the ground-truth values for  $\mu_0^1$ ,  $\gamma^1$ ,  $\alpha^{1,f}$ , and  $\nu^{1,f}$  respectively. The estimated parameters are reasonably robust and centered around the ground-truth values. In addition, we plot the log-likelihood functions with respect to changes in the parameter value. We observe that the log-likelihood functions are well-behaved and maximized by the ground-truth parameter values, with the exception of  $\gamma$ . The log-likelihood function value is insensitive to changes in  $\gamma^1$  over a certain range, displaying sloppiness [63].

---

<sup>4</sup><https://x-datainitiative.github.io/tick/index.html>

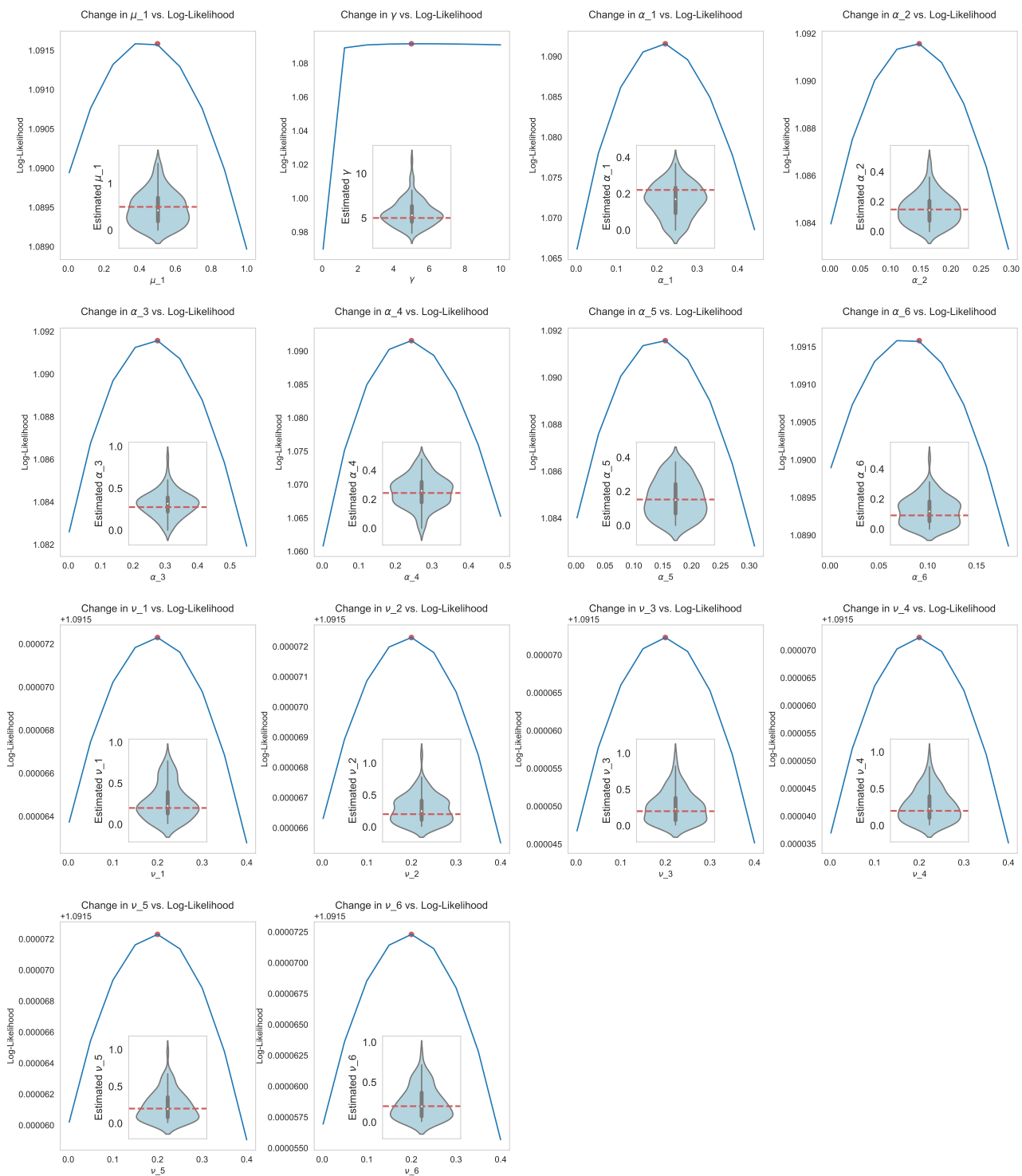


Figure H.1: We plot the shape of the log-likelihood function in Equation (9) varying the target parameter while holding the other parameters fixed at their ground-truth values. The ground-truth values of the target parameter are indicated by the red dots. The log-likelihood values are normalized by the number of events  $N^e$  to be comparable across varying numbers of data points. The inset plots show the distribution of the fitted parameters from 100 bootstrapped samples. The red dashed lines indicate the ground-truth values for the parameter of interest. We show results for the first process in a 6-dimensional multivariate Hawkes process. The other processes have comparable performances.